Shielding of Multi-Leg Penetrations into the RHIC Collider

Brookhaven National Laboratory

MEMORANDUM

Date: 08/28/98

To: S. Musolino

From: A.J. Stevens AJS

Subj.: Dose at Exit of Duct Covers

As you are well aware, the degree of access restriction required near the exits of vent ducts has not yet been finalized. My scaling of Gollon's estimates[1] was based on what I believe was an underestimate of the source term used. Another aspect which might be taken into account in deciding the access restrictions necessary is the fact that every vent has a cover which extends beyond the exterior of the berm, whereas Gollon took his last leg only to that point.[2] If each vent stack is assumed to extend 3 ft. above the berm, the added length reduces the "exit dose" by a factor of between 1.7 and 2.0[3] I show below a spreadsheet table as given in Ref. [1], but with an added column labeled "Dose at Cover."

	Emergency Exhaust Ducts by Archetype				
Vent Case	*Source*	*Leg 1*	*Leg 2*	*Exit Dose*	*Dose at Cover*
	(rem)			(rem)	(rem)
A	540.0	1.29E-01	6.56E-04	0.046	0.027
B-1	996.0	1.11E-01	4.40E-03	0.486	0.270
B-2	996.0	1.23E-01	6.78E-03	0.831	0.475
C	676.0	1.35E-01	5.56E-03	0.507	0.298
D-1	676.0	1.23E-01	2.59E-03	0.215	0.119
D-2	368.0	1.55E-01	4.17E-03	0.238	0.136
E	762.0	1.31E-01	5.56E-03	0.555	0.326
F-1	468.0	1.46E-01	5.56E-03	0.396	0.192
F-2	240.0	1.66E-01	5.56E-03	0.224	0.132
G-1	716.0	1.33E-01	5.56E-03	0.529	0.311
G-2	468.0	1.46E-01	5.56E-03	0.396	0.233
H	468.0	1.32E-01	2.88E-03	0.186	0.103
I-1	204.0	1.57E-01	1.61E-02	0.516	0.258
I-2	204.0	1.73E-01	2.27E-02	0.801	0.411
J-1	190.8	5.53E-02	7.72E-03	0.081	0.042
J-2	190.8	6.89E-02	1.14E-02	0.150	0.083

These estimates (which assume ½ of 4 times design intensity loss and × 2 neutron QF) are obtained by applying labyrinth formula to an entrance dose derived from a simple CASIM calculation; no "punch through" is included. A more recent Monte Carlo calculation[4] using the Lahet Code System and a 3-D CASIM geometry, which should in principle over-estimate the dose, obtained 550 ± 27 mrem (statistical error only) at the cover for vent case B-2.

References

1. Memorandum from A.J. Stevens to S. Musolino dated 08/26/97, Subj: "Scaling Follon's Duct and Labyrinth Calculations."

2. P.J. Gollon, "Shielding of Multi-Leg Penetrations into the RHIC Collider," AD/RHIC/RD-76, October, 1994. See Fig. 6 in this Reference.

3. For the scaling the formula of Goebel (non first leg) given in Ref. [2] is used. The attenuation is given by $1 + 2.8d(1.57)^{d+2}$ where d is $L/\sqrt{A}$, L and A being the leg length and cross sectional area.

4. A.J. Stevens, "Improved Estimation of Dose Near Vent Exits in the RHIC Collider Tunnel," (to be published as a RHIC R&D note).

Brookhaven National Laboratory

MEMORANDUM

DETECTOR RHIC GROUP

Date: 08/26/97

To: S. Musolino

From: A.J. Stevens ajs

Subj.: Scaling Gollon's Duct and Labyrinth Calculations

As you know, I recently used the LAHET Code System (LCS) to calculate the dose at the exit of two multi-leg penetrations, one duct (or vent) and one labyrinth.[1] The results were considerably higher than the estimates of Gollon.[2]

I believe that most of the discrepancy lies in two approximations made by Gollon that are not verified by the LCS results. On Page 8 of Ref. [2], one finds the following statement: "Since the CASIM conversion factor from star density to dose equivalent...incorporates the omni-directional low energy neutrons that come from backscattering from the accelerator enclosure wall, this empirical correction factor of two is not necessary." The factor of two referred to is in the Tesch formula which explicitly multiplies the dose from a point source to account for albedo from the enclosure. The calculations of Ref. [1] would indicate that *at least* a factor of 2 is required in the "typical" RHIC tunnel. The second approximation is found on page 10 of Ref. [2]. In referring to the effect of a distributed source on the Tesch formula, Gollon states "The magnitude of this effect is somewhat arbitrarily taken to be 0.25 for all cases in which the beamline is within 25 degrees of the axis of the first leg." Now the source is "distributed" in more than one sense, but the LCS results indicate that the reduction factor applied by Gollon was too great, especially for the labyrinths where the opening is typically larger than the source length if the latter object is simply considered to be the ~ 1m length of a quadrupole.

I have scaled Gollon's spreadsheet results in the following manner. First, I have multiplied the entrance fault dose by a factor of 2 for the backscatter. Secondly, for ducts whose first leg axis is within 25° of the beamline, I have taken the first leg attenuation to be the geometric mean between the Tesch formula and the Goebel formula. This still allows for some reduction for a "distributed source," but less (by a factor of 2) than allowed by Gollon. For ducts further off the beamline I simply use the Goebel first leg formula. In labyrinths (all of which have first leg "openings" as large or larger than the source length), I use the Tesch formula (with no reduction) for the first leg and the Goebel formula for subsequent legs.

The results are shown in Tables 1 through 3 which are attached. Entries which have an asterisk in the column labeled "case" are in experimental halls. In general these should not be considered since the halls are considered separately. An example is personnel access case P-18,

which is not being used for personnel access and is shadowed by shielding blocks in the STAR shielding design. One personnel access considered by Gollon, case P-2, does not appear in Table 1. This is the curved labyrinth at the injection line split. The geometry here is totally different from that considered in Ref. [1], so no "lessons learned" can be applied.

Note that the factor of 2 multiplier for an assumed increase in the neutron quality factor is still applied in these tables. The cases calculated in Ref. [1] correspond to case V-7 in Table 2 (677 mrem.) or archetype B-2 in Table 3 (831 mrem.). In these units, the result of Ref. [1] would be 1001 ± 215 mrem. The labyrinth calculated in Ref. [1] was case P-8. Again, with the factor of 2 QF increase, the LCS result of 24 ± 3 mrem. compares to the scaled result in Table 1 of 13 mrem.

This scaling is certainly too simplistic. However, the two reduction factors applied by Gollon are (in hindsight) very difficult to justify, so that the estimates in the attached tables represent at least *improved* estimates when compared to the original spread sheet values. In examining the numbers in the attached tables I note the following.

Personnel Access Labyrinths

With the exception of case P-11, a labyrinth at 10 o'clock which is, in fact, being re-built, the fault estimates are well below 100 mrem. I believe the exits for all there labyrinths are in controlled areas (radiation training and badges required) where the criteria for such a fault is 1000 mrem. Hence, the re-estimate in these cases is not relevant. [One personnel labyrinth - at 8 o'clock where a collimator is a nearby source of "normal loss" - will need to be considered in future LCS calculations.]

Ducts

Most of the ducts have exit doses which exceed the low occupancy criteria of 160 mrem. In many cases (Archetypes B-2 and I-2 which are numerous) this was true in the case of Gollon's estimates. The LCS calculation in Ref. [1] for a point 2 ft. away from the side of one of the B-2 vents gave a result of 54 ± 45 mrem. excess dose if the neutron quality factor is multiplied by 2. If one conservatively adds this to the CASIM no-hole dose, the total would be about the 160 mrem. criteria. The LCS calculation is clearly not definitive here, and might be improved with additional calculations. However, two issues (which may be correlated) associated with at least those ducts whose first leg points directly at the lattice magnets must be given further attention.

1. If the neutron QF is doubled, the fact that a point 2 ft. away is "close to" 160 mrem. may imply either the necessity or desirability of an access-restricting structure/posting more than 2 ft. away from the side of the ducts.

2. Without regard to the QF being doubled, the DBA fault dose estimate *on top of* the duct covers will exceed 160 mrem. However, if the QF is doubled the dose may be "close to" 1 rem.

which is the criteria for a fault in a controlled area. The issue here is whether the duct structures themselves are sufficient barriers and, if not, what further structures are required.

References

1. A.J. Stevens, "Comparison of CASIM with the LAHET Code System," AD/RHIC/RD-115, August 1997.

2. P.J. Gollon, "Shielding of Multi-Leg Penetrations into the RHIC Collider," AD/RHIC/RD-76, October, 1994.

Attachments

Personnel Access Labyrinths					
Case	*Source* (rem)	*Leg 1*	*Leg 2*	*Leg 3*	*Exit Dose* (rem)
P-1	97.4	9.00E-02	1.29E-02	1.04E-02	0.001
P-3	364.0	1.11E-01	3.69E-02	4.56E-03	0.007
P-4	440.0	1.19E-01	5.93E-03	2.24E-01	0.070
P-5	364.0	2.50E-01	2.77E-02	1.31E-02	0.033
P-6	260.0	2.50E-01	5.55E-02	5.20E-03	0.019
P-7	440.0	1.89E-01	5.55E-02	3.40E-03	0.016
P-8	686.0	5.54E-02	1.84E-02	1.84E-02	0.013
P-9	440.0	1.98E-01	5.81E-02	7.03E-03	0.036
P-10	260.0	9.45E-02	2.84E-02	2.85E-03	0.002
P-11	260.0	4.00E-02	2.60E-02	None	0.270
P-12	224.0	8.87E-02	3.61E-02	4.86E-03	0.003
P-14	224.0	8.87E-02	1.13E-02	4.68E-02	0.011
P-15	440.0	1.48E-01	5.55E-02	5.80E-03	0.021
P-16	39.6	1.32E-01	3.69E-02	3.99E-02	0.008
P-17	440.0	1.94E-01	5.81E-02	4.84E-03	0.024
P-18(*)	27.4	7.56E-01	2.88E-02	None	0.597
P-19	542.0	7.01E-02	3.69E-02	4.27E-02	0.060

Table 1

Emergency Exhaust Ducts				
Case	***Source*** (rem)	***Leg 1***	***Leg 2***	***Exit Dose*** (rem)
V-2	254.0	9.61E-02	2.26E-03	0.055
V-3	318.0	6.50E-02	8.02E-03	0.166
V-4	168.8	5.33E-02	1.42E-02	0.128
V-5	168.8	5.33E-02	1.42E-02	0.128
V-6	168.8	1.35E-01	2.11E-02	0.481
V-7	868.0	1.27E-01	6.14E-03	0.677
V-8	762.0	1.19E-01	3.95E-03	0.358
V-9	1.4	7.71E-02	4.50E-03	0.000
V-10	540.0	1.29E-01	3.95E-03	0.275
V-11	996.0	1.23E-01	6.14E-03	0.752
V-12	488.0	1.32E-01	9.60E-04	0.062
V-13a	122.0	1.36E-01	2.01E-03	0.033
V-13b	122.0	4.18E-02	2.92E-02	0.149
V-14	488.0	2.07E-02	2.16E-03	0.022
V-15	122.0	8.46E-02	7.20E-03	0.074
V-16	488.0	1.46E-01	2.01E-03	0.143
V-17	488.0	1.22E-01	7.49E-03	0.446
V-18	488.0	1.22E-01	7.49E-03	0.446
V-19	488.0	1.22E-01	7.49E-03	0.446
V-20	368.0	1.16E-01	2.11E-03	0.090
V-21	168.8	4.18E-02	9.77E-03	0.069
V-22	190.6	1.48E-01	2.92E-02	0.824
V-23	540.0	1.42E-01	6.14E-03	0.471
V-24	122.0	4.18E-02	1.42E-03	0.007
V-25	122.0	1.31E-01	1.42E-03	0.023
V-26	488.0	1.22E-01	1.42E-02	0.845
V-27	168.8	1.51E-01	1.42E-02	0.362
V-28	168.8	5.33E-02	1.42E-02	0.128
V-29	488.0	1.57E-01	4.35E-03	0.333
V-30	488.0	1.46E-01	4.17E-03	0.297
V-31(*)	78.0	6.99E-02	1.07E-04	0.001
V-32(*)	78.0	3.76E-02	1.93E-02	0.057
V-33(*)	78.0	3.76E-02	1.86E-04	0.001
V-34(*)	54.2	1.49E-01	2.13E-01	1.720
V-35(*)	54.2	8.00E-02	8.24E-04	0.004

Table 2

Emergency Exhaust Ducts by Archetype				
Vent Case	*Source* (rem)	*Leg 1*	*Leg 2*	*Exit Dose* (rem)
A	540.0	1.29E-01	6.56E-04	0.046
B-1	996.0	1.11E-01	4.40E-03	0.486
B-2	996.0	1.23E-01	6.78E-03	0.831
C	676.0	1.35E-01	5.56E-03	0.507
D-1	676.0	1.23E-01	2.59E-03	0.215
D-2	368.0	1.55E-01	4.17E-03	0.238
E	762.0	1.31E-01	5.56E-03	0.555
F-1	488.0	1.46E-01	5.56E-03	0.396
F-2	240.0	1.68E-01	5.56E-03	0.224
G-1	716.0	1.33E-01	5.56E-03	0.529
G-2	488.0	1.46E-01	5.56E-03	0.396
H	488.0	1.32E-01	2.88E-03	0.186
I-1	204.0	1.57E-01	1.61E-02	0.516
I-2	204.0	1.73E-01	2.27E-02	0.801
J-1	190.6	5.53E-02	7.72E-03	0.081
J-2	190.6	6.89E-02	1.14E-02	0.150

Table 3

AD/RHIC/RD–76A

RHIC PROJECT

Brookhaven National Laboratory

Amendment to Shielding of Multi-Leg Penetrations into the RHIC Collider

Peter J. Gollon

July 1996

RHIC EMERGENCY EXHAUST DUCTS, geometry details

Case	Archetype Description	Comment	Dia (in)	Distance to beam (ft)	Vert pipe length (ft)	Source Angle (deg)
A	Sext 3 Conc Struct at Spect Tunnel		42	9.5	25.0	0
B-1	16 FT PLATE ARCH		42	7.0	15.5	0
B-2	16 FT PLATE ARCH		48	7.0	15.5	0
C	20 FT PLATE ARCH		48	8.5	16.5	0
D-1	26 FT PLATE ARCH		42	8.5	18.0	0
D-2	26 FT PLATE ARCH		48	11.5	18.0	0
E	CONC STRUCT @ 4 o'clock		48	8.0	16.5	0
F-1	INJ-EJECT AT SEXT 5,7	Near Wall	48	10.0	16.5	0
F-2	INJ-EJECT AT SEXT 5,7	Far Wall	48	14.3	16.5	0
G-1	INJ/EJCTS AT WIDE ANGL	Near Wall	48	8.3	16.5	0
G-2	INJ/EJCTS AT WIDE ANGL	Far Wall	48	10.0	16.5	0
H	RF CAVITY SEXT. 5		42	10.0	17.5	0
I-1	ALCOVE A AND C - TYPICAL		42	15.5	10.0	15
I-2	ALCOVE A AND C - TYPICAL		48	15.5	10.0	15
J-1	ALCOVE B - TYPICAL		42	16.0	13.0	50
J-2	ALCOVE B - TYPICAL		48	16.0	13.0	50

RHIC EMERGENCY EXHAUST DUCTS, sorted by case

Case	Archetype Description	Dia, in	Sext	Project	Dwg	Comment
A	Sext 3 Conc Struct at Spect Tı	42	3	ISA	S - 2/20 - 13	
		42	3	ISA	A - 4/9 - 13	
		42	3	ISA	A - 7/12 - 13	
B-1	16 FT PLATE ARCH	42	1	ISA	S - 1/56 - 4	
		42	1	ISA	S - 4/59 - 4	
		42	3	ISA	S - 8/63 - 4	
		42	7	ISA	S - 8/62 - 2	
		42	9	ISA	S - 1/56 - 11	
		42	9	ISA	S - 4/59 - 11	
		42	11	RHIC	S - 2/125 -	
		42	11	ISA	S - 5/60 - 11	
		42	11	ISA	S - 8/63 - 11	
		42	3	ISA	S - 5/60 - 4	
		42	3	ISA	S - 5/61 - 4	
B-2		48	1	ISA	S - 2/57 - 4	
		48	1	ISA	S - 3/58 - 4	
		48	3	ISA	S - 6/61 - 4	
		48	3	ISA	S - 7/62 -4	
		48	5	ISA	S - 2/56 - 2	
		48	5	ISA	S - 3/57 - 2	
		48	7	ISA	S - 7/61 - 2	
		48	7	ISA		
		48	9	ISA	S - 2/57 - 11	
		48	9	ISA	S - 3/58 - 11	
		48	11	ISA	S - 6/61 - 11	
		48	11	ISA	S - 7/61 - 11	
C	20 FT PLATE ARCH	48	7	ISA	S - 2/25 - 18	
		48	9	ISA	S - 2/25 - 18	
		48	1	ISA	S - 2/20 - 13	
D-1	26 FT PLATE ARCH	42	11	RHIC	S - 14/75	
D-2		48	1	RHIC	S - 34/75	
		48	9	RHIC	S - 1/125	
E	CONC STRUCT @ 4 o'clock	48	5		S - 1/17 - 10	
	view looking west	48	3		S - 1/17 - 10	
F-1	INJ-EJECT AT SEXT 5,7	48	5		A - 4/16 - 15	NEAR WALL
	view looking west	48	7		A - 3/15 - 15	NEAR WALL
F-2	INJ-EJECT AT SEXT 5,7	48	5		A - 4/16 - 15	FAR WALL
	view looking west	48	7		A - 3/15 - 15	FAR WALL
G-1	INJ/EJCTS AT WIDE ANGLE	48	5		A - 4/16 - 15	NEAR WALL
	view looking east	48	7		A - 3/15 - 15	NEAR WALL
G-2	INJ/EJCTS AT WIDE ANGLE	48	5		A - 4/16 - 15	FAR WALL
	view looking east	48	7		A - 3/15 - 15	FAR WALL
H	RF CAVITY SEXT. 5	42	5		S - 1/55 - 2	

RHIC EMERGENCY EXHAUST DUCTS, sorted by case

Case	Archetype Description	Dia, in	Sext	Project Dwg	Comment
I-1	ALCOVE A AND C - TYPICAL	42	3	S - 7/62 - 4	Alcove C
		42	7	S - 7/61 - 2	Alcove C
		42	1	S - 3/58 - 4	Alcove C
		42	7	S - 6/60 - 2	Alcove A
		42	1	S - 2/57 - 4	Alcove A
		42	3	S - 6/61 - 4	Alcove A
		42	5	S - 3/57 - 2	Alcove C
I-2		48	11	S - 7/62 - 11	Alcove C
		48	9	S - 3/58 - 11	Alcove C
		48	5	S - 2/56 - 2	Alcove A
		48	9	S - 2/57 - 11	Alcove A
		48	11	S - 6/61 - 11	Alcove A
J-1	ALCOVE B - TYPICAL	42	5	S - 2/56 - 2	
		42	7	S - 6/60 - 2	
J-2		48	1	S - 2/57 - 4	
		48	3	S - 6/61 - 4	
		48	9	S - 2/57 - 11	
		48	11	S - 6/61 - 11	

RHIC EMERGENCY EXHAUST DUCTS

Case	Archetype Description	Dia, in	Sext	Project	Dwg	Comment
A	Sext 3 Conc Struct at Spect Tu	42	3	ISA	S - 2/20 - 13	
		42	3	ISA	A - 4/9 - 13	
		42	3	ISA	A - 7/12 - 13	
B-1a	16 FT PLATE ARCH	42	1	ISA	S - 1/56 - 4	
		42	1	ISA	S - 4/59 - 4	
		42	3	ISA	S - 8/63 - 4	
		42	7	ISA	S - 8/62 - 2	
		42	9	ISA	S - 1/56 - 11	
		42	9	ISA	S - 4/59 - 11	
		42	11	RHIC	S - 2/125 -	
		42	11	ISA	S - 5/60 - 11	
		42	11	ISA	S - 8/63 - 11	
B-1	16 FT PLATE ARCH	42	3	ISA	S - 5/60 - 4	
		42	3	ISA	S - 5/61 - 4	
B-2		48	1	ISA	S - 2/57 - 4	
		48	1	ISA	S - 3/58 - 4	
		48	3	ISA	S - 6/61 - 4	
		48	3	ISA	S - 7/62 -4	
		48	5	ISA	S - 2/56 - 2	
		48	5	ISA	S - 3/57 - 2	
		48	7	ISA	S - 7/61 - 2	
		48	7	ISA		
		48	9	ISA	S - 2/57 - 11	
		48	9	ISA	S - 3/58 - 11	
		48	11	ISA	S - 6/61 - 11	
		48	11	ISA	S - 7/61 - 11	
C	20 FT PLATE ARCH	48	7	ISA	S - 2/25 - 18	
		48	9	ISA	S - 2/25 - 18	
		48	1	ISA	S - 2/20 - 13	
D-1	26 FT PLATE ARCH	42	11	RHIC	S - 14/75	
D-2		48	1	RHIC	S - 34/75	
		48	9	RHIC	S - 1/125	
E	CONC STRUCT @ 4 o'clock	48	5		S - 1/17 - 10	
	view looking west	48	3		S - 1/17 - 10	
F-1	INJ-EJECT AT SEXT 5,7	48	5		A - 4/16 - 15	NEAR WALL
	view looking west	48	7		A - 3/15 - 15	NEAR WALL
F-2	INJ-EJECT AT SEXT 5,7	48	5		A - 4/16 - 15	FAR WALL
	view looking west	48	7		A - 3/15 - 15	FAR WALL
G-1	INJ/EJCTS AT WIDE ANGLE	48	5		A - 4/16 - 15	NEAR WALL
	view looking east	48	7		A - 3/15 - 15	NEAR WALL
G-2	INJ/EJCTS AT WIDE ANGLE	48	5		A - 4/16 - 15	FAR WALL
	view looking east	48	7		A - 3/15 - 15	FAR WALL
H	RF CAVITY SEXT. 5	42	5		S - 1/55 - 2	
I-1,I-2	ALCOVE A AND C - TYPICAL	42	1		S - 2/57 - 4	Alcove A
		42	3		S - 6/61 - 4	Alcove A
		48	5		S - 2/56 - 2	Alcove A
		42	7		S - 6/60 - 2	Alcove A
		48	9		S - 2/57 - 11	Alcove A
		48	11		S - 6/61 - 11	Alcove A
		42	1		S - 3/58 - 4	Alcove C

RHIC EMERGENCY EXHAUST DUCTS

	42	3	S - 7/62 - 4	Alcove C
	42	5	S - 3/57 - 2	Alcove C
	42	7	S - 7/61 - 2	Alcove C
	48	9	S - 3/58 - 11	Alcove C
	48	11	S - 7/62 - 11	Alcove C
J-1,J-2 ALCOVE B - TYPICAL	48	1	S - 2/57 - 4	
	48	3	S - 6/61 - 4	
	42	5	S - 2/56 - 2	
	42	7	S - 6/60 - 2	
	48	9	S - 2/57 - 11	
	48	11	S - 6/61 - 11	

RHIC EMERGENCY EXHAUST DUCTS, archetype results

Vent Case	**A**	
Location	Sext 3 Conc Struct at Spect Tunnel	
Geometry Comments		

		Leg 1	Leg 2
GEOMETRY DATA:			
INPUT	dist to Beam (ft)	9.50	
	pipe dia (in)	42.00	
	horiz. pipe length, d1 (ft)	6.00	
	vertical CL length, d2 (ft)		25.00
METRIC	distance to beam, a (m)	2.90	
	horiz. pipe length, d1 (m)	1.83	
	vertical CL pipe length, d2 (m)		7.62
	pipe dia (m)	1.07	1.07
	pipe area, A (sq m)	0.89	0.89
LEG LENGTHS (meters):			
	Leg 1 length to mid-bend, R1 (m)	2.36	
TESCH	Leg 1: Source to mid-bend, r1 = R1 + a	5.26	
TESCH	Leg 2, length from leg 1 pipe, R2		7.09
GOEBEL	Leg length, Ri/Sqrt(A)	2.50	7.50
ATTENUATION DETAILS:			
TESCH	Tesch leg atten	3.03E-01	1.83E-03
	Tesch vent attenuation:		5.55E-04
	Angle, source to leg 1 axis (deg)		0
	Source Geometry Effect		0.250
	Total Tesch Vent Attenuation		1.39E-04
GOEBEL	Goebel leg atten	5.53E-02	6.56E-04
	Total Goebel Vent Attenuation		3.63E-05
MEAN	Geometric Mean Vent Attenuation		7.09E-05
	"Variance" factor:		1.95
SOURCE TERM:			
	No. of ions lost		1.14E+11
	Std star per cc/ion lost		1.35E-04
	Dose-Equiv (rem) per star		2.66E-05
	Low Energy Fraction		0.85
	Entrance Dose-Equiv (rem)		2.70E+02
OVERALL RESULT:			
	Exit Dose (rem) [Tesch]		3.75E-02
	Exit Dose (rem) [Goebel]		9.80E-03
	Geometric Mean		*1.92E-02*

RHIC EMERGENCY EXHAUST DUCTS, archetype results

Vent Case	**B-1**	
Location	16 FT PLATE ARCH	
Geometry Comments		

		Leg 1	Leg 2
GEOMETRY DATA:			
INPUT	dist to Beam (ft)	7.00	
	pipe dia (in)	42.00	
	horiz. pipe length, d1 (ft)	6.00	
	vertical CL length, d2 (ft)		15.50
METRIC	distance to beam, a (m)	2.13	
	horiz. pipe length, d1 (m)	1.83	
	vertical CL pipe length, d2 (m)		4.72
	pipe dia (m)	1.07	1.07
	pipe area, A (sq m)	0.89	0.89
LEG LENGTHS (meters):			
	Leg 1 length to mid-bend, R1 (m)	2.36	
TESCH	Leg 1: Source to mid-bend, r1 = R1 + a	4.50	
TESCH	Leg 2, length from leg 1 pipe, R2		4.19
GOEBEL	Leg length, Ri/Sqrt(A)	2.50	4.43
ATTENUATION DETAILS:			
TESCH	Tesch leg atten	2.25E-01	6.44E-03
	Tesch vent attenuation:		1.45E-03
	Angle, source to leg 1 axis (deg)		0
	Source Geometry Effect		0.250
	Total Tesch Vent Attenuation		3.63E-04
GOEBEL	Goebel leg atten	5.53E-02	4.40E-03
	Total Goebel Vent Attenuation		2.43E-04
MEAN	Geometric Mean Vent Attenuation		2.97E-04
	"Variance" factor:		1.22

SOURCE TERM:		
	No. of ions lost	1.14E+11
	Std star per cc/ion lost	1.35E-04
	Dose-Equiv (rem) per star	2.66E-05
	Low Energy Fraction	0.85
	Entrance Dose-Equiv (rem)	4.98E+02
OVERALL RESULT:		
	Exit Dose (rem) [Tesch]	1.81E-01
	Exit Dose (rem) [Goebel]	1.21E-01
	Geometric Mean	*1.48E-01*

RHIC EMERGENCY EXHAUST DUCTS, archetype results

	Vent Case	**B-2**
	Location	16 FT PLATE ARCH
	Geometry Comments	

		Leg 1	Leg 2
GEOMETRY DATA:			
INPUT	dist to Beam (ft)	7.00	
	pipe dia (in)	48.00	
	horiz. pipe length, d1 (ft)	6.00	
	vertical CL length, d2 (ft)		15.50
METRIC	distance to beam, a (m)	2.13	
	horiz. pipe length, d1 (m)	1.83	
	vertical CL pipe length, d2 (m)		4.72
	pipe dia (m)	1.22	1.22
	pipe area, A (sq m)	1.17	1.17
LEG LENGTHS (meters):			
	Leg 1 length to mid-bend, R1 (m)	2.44	
TESCH	Leg 1: Source to mid-bend, r1 = R1 + a	4.57	
TESCH	Leg 2, length from leg 1 pipe, R2		4.11
GOEBEL	Leg length, R/Sqrt(A)	2.26	3.81
ATTENUATION DETAILS:			
TESCH	Tesch leg atten	2.18E-01	9.30E-03
	Tesch vent attenuation:		2.03E-03
	Angle, source to leg 1 axis (deg)		0
	Source Geometry Effect		0.250
	Total Tesch Vent Attenuation		5.06E-04
GOEBEL	Goebel leg atten	6.89E-02	6.78E-03
	Total Goebel Vent Attenuation		4.67E-04
MEAN	Geometric Mean Vent Attenuation		4.86E-04
	"Variance" factor:		1.04
SOURCE TERM:			
	No. of ions lost		1.14E+11
	Std star per cc/ion lost		1.35E-04
	Dose-Equiv (rem) per star		2.66E-05
	Low Energy Fraction		0.85
	Entrance Dose-Equiv (rem)		4.98E+02
OVERALL RESULT:			
	Exit Dose (rem) [Tesch]		2.52E-01
	Exit Dose (rem) [Goebel]		2.32E-01
	Geometric Mean		*2.42E-01*

RHIC EMERGENCY EXHAUST DUCTS, archetype results

	Vent Case	**C**
	Location	20 FT PLATE ARCH
	Geometry Comments	

		Leg 1	Leg 2
GEOMETRY DATA:			
INPUT	dist to Beam (ft)	8.50	
	pipe dia (in)	48.00	
	horiz. pipe length, d1 (ft)	6.00	
	vertical CL length, d2 (ft)		16.50
METRIC	distance to beam, a (m)	2.59	
	horiz. pipe length, d1 (m)	1.83	
	vertical CL pipe length, d2 (m)		5.03
	pipe dia (m)	1.22	1.22
	pipe area, A (sq m)	1.17	1.17
LEG LENGTHS (meters):			
	Leg 1 length to mid-bend, R1 (m)	2.44	
TESCH	Leg 1: Source to mid-bend, r1 = R1 + a	5.03	
TESCH	Leg 2, length from leg 1 pipe, R2		4.42
GOEBEL	Leg length, Ri/Sqrt(A)	2.26	4.09
ATTENUATION DETAILS:			
TESCH	Tesch leg atten	2.65E-01	8.09E-03
	Tesch vent attenuation:		2.15E-03
	Angle, source to leg 1 axis (deg)		0
	Source Geometry Effect		0.250
	Total Tesch Vent Attenuation		5.37E-04
GOEBEL	Goebel leg atten	6.89E-02	5.56E-03
	Total Goebel Vent Attenuation		3.83E-04
MEAN	Geometric Mean Vent Attenuation		4.53E-04
	"Variance" factor:		1.18

SOURCE TERM:		
	No. of ions lost	1.14E+11
	Std star per cc/ion lost	1.35E-04
	Dose-Equiv (rem) per star	2.66E-05
	Low Energy Fraction	0.85
	Entrance Dose-Equiv (rem)	3.38E+02
OVERALL RESULT:		
	Exit Dose (rem) [Tesch]	1.81E-01
	Exit Dose (rem) [Goebel]	1.29E-01
	Geometric Mean	*1.53E-01*

RHIC EMERGENCY EXHAUST DUCTS, archetype results

Vent Case	**D-1**	
Location	26 FT PLATE ARCH	
Geometry Comments		

		Leg 1	Leg 2
GEOMETRY DATA:			
INPUT	dist to Beam (ft)	8.50	
	pipe dia (in)	42.00	
	horiz. pipe length, d1 (ft)	6.00	
	vertical CL length, d2 (ft)		18.00
METRIC	distance to beam, a (m)	2.59	
	horiz. pipe length, d1 (m)	1.83	
	vertical CL pipe length, d2 (m)		5.49
	pipe dia (m)	1.07	1.07
	pipe area, A (sq m)	0.89	0.89
LEG LENGTHS (meters):			
	Leg 1 length to mid-bend, R1 (m)	2.36	
TESCH	Leg 1: Source to mid-bend, r1 = R1 + a	4.95	
TESCH	Leg 2, length from leg 1 pipe, R2		4.95
GOEBEL	Leg length, R/Sqrt(A)	2.50	5.24
ATTENUATION DETAILS:			
TESCH	Tesch leg atten	2.74E-01	4.56E-03
	Tesch vent attenuation:		1.25E-03
	Angle, source to leg 1 axis (deg)		0
	Source Geometry Effect		0.250
	Total Tesch Vent Attenuation		3.12E-04
GOEBEL	Goebel leg atten	5.53E-02	2.59E-03
	Total Goebel Vent Attenuation		1.43E-04
MEAN	Geometric Mean Vent Attenuation		2.12E-04
	"Variance" factor:		1.48
SOURCE TERM:			
	No. of ions lost		1.14E+11
	Std star per cc/ion lost		1.35E-04
	Dose-Equiv (rem) per star		2.66E-05
	Low Energy Fraction		0.85
	Entrance Dose-Equiv (rem)		3.38E+02
OVERALL RESULT:			
	Exit Dose (rem) [Tesch]		1.05E-01
	Exit Dose (rem) [Goebel]		4.64E-02
	Geometric Mean		*7.14E-02*

RHIC EMERGENCY EXHAUST DUCTS, archetype results

Vent Case		**D-2**
Location		26 FT PLATE ARCH
Geometry Comments		

		Leg 1	Leg 2
GEOMETRY DATA:			
INPUT	dist to Beam (ft)	11.50	
	pipe dia (in)	48.00	
	horiz. pipe length, d1 (ft)	6.00	
	vertical CL length, d2 (ft)		18.00
METRIC	distance to beam, a (m)	3.51	
	horiz. pipe length, d1 (m)	1.83	
	vertical CL pipe length, d2 (m)		5.49
	pipe dia (m)	1.22	1.22
	pipe area, A (sq m)	1.17	1.17
LEG LENGTHS (meters):			
	Leg 1 length to mid-bend, R1 (m)	2.44	
TESCH	Leg 1: Source to mid-bend, r1 = R1 + a	5.94	
TESCH	Leg 2, length from leg 1 pipe, R2		4.88
GOEBEL	Leg length, Ri/Sqrt(A)	2.26	4.51
ATTENUATION DETAILS:			
TESCH	Tesch leg atten	3.48E-01	6.61E-03
	Tesch vent attenuation:		2.30E-03
	Angle, source to leg 1 axis (deg)		0
	Source Geometry Effect		0.250
	Total Tesch Vent Attenuation		5.75E-04
GOEBEL	Goebel leg atten	6.89E-02	4.17E-03
	Total Goebel Vent Attenuation		2.87E-04
MEAN	Geometric Mean Vent Attenuation		4.06E-04
	"Variance" factor:		1.41

SOURCE TERM:		
	No. of ions lost	1.14E+11
	Std star per cc/ion lost	1.35E-04
	Dose-Equiv (rem) per star	2.66E-05
	Low Energy Fraction	0.85
	Entrance Dose-Equiv (rem)	1.84E+02
OVERALL RESULT:		
	Exit Dose (rem) [Tesch]	1.06E-01
	Exit Dose (rem) [Goebel]	5.30E-02
	Geometric Mean	7.49E-02

RHIC EMERGENCY EXHAUST DUCTS, archetype results

	Vent Case	**E**
	Location	CONC STRUCT @ 4 o'clock
	Geometry Comments	

		Leg 1	Leg 2
GEOMETRY DATA:			
INPUT	dist to Beam (ft)	8.00	
	pipe dia (in)	48.00	
	horiz. pipe length, d1 (ft)	6.00	
	vertical CL length, d2 (ft)		16.50
METRIC	distance to beam, a (m)	2.44	
	horiz. pipe length, d1 (m)	1.83	
	vertical CL pipe length, d2 (m)		5.03
	pipe dia (m)	1.22	1.22
	pipe area, A (sq m)	1.17	1.17
LEG LENGTHS (meters):			
	Leg 1 length to mid-bend, R1 (m)	2.44	
TESCH	Leg 1: Source to mid-bend, r1 = R1 + a	4.88	
TESCH	Leg 2, length from leg 1 pipe, R2		4.42
GOEBEL	Leg length, Ri/Sqrt(A)	2.26	4.09
ATTENUATION DETAILS:			
TESCH	Tesch leg atten	2.50E-01	8.09E-03
	Tesch vent attenuation:		2.02E-03
	Angle, source to leg 1 axis (deg)		0
	Source Geometry Effect		0.250
	Total Tesch Vent Attenuation		5.06E-04
GOEBEL	Goebel leg atten	6.89E-02	5.56E-03
	Total Goebel Vent Attenuation		3.83E-04
MEAN	Geometric Mean Vent Attenuation		4.40E-04
	"Variance" factor:		1.15
SOURCE TERM:			
	No. of ions lost		1.14E+11
	Std star per cc/ion lost		1.35E-04
	Dose-Equiv (rem) per star		2.66E-05
	Low Energy Fraction		0.85
	Entrance Dose-Equiv (rem)		3.81E+02
OVERALL RESULT:			
	Exit Dose (rem) [Tesch]		1.93E-01
	Exit Dose (rem) [Goebel]		1.46E-01
	Geometric Mean		*1.68E-01*

RHIC EMERGENCY EXHAUST DUCTS, archetype results

	Vent Case	**F-1**
	Location	INJ-EJECT AT SEXT 5,7
	Geometry Comments	Near Wall

		Leg 1	Leg 2
GEOMETRY	**DATA:**		
INPUT	dist to Beam (ft)	10.00	
	pipe dia (in)	48.00	
	horiz. pipe length, d1 (ft)	6.00	
	vertical CL length, d2 (ft)		16.50
METRIC	distance to beam, a (m)	3.05	
	horiz. pipe length, d1 (m)	1.83	
	vertical CL pipe length, d2 (m)		5.03
	pipe dia (m)	1.22	1.22
	pipe area, A (sq m)	1.17	1.17
LEG LENGTHS (meters):			
	Leg 1 length to mid-bend, R1 (m)	2.44	
TESCH	Leg 1: Source to mid-bend, r1 = R1 + a	5.49	
TESCH	Leg 2, length from leg 1 pipe, R2		4.42
GOEBEL	Leg length, Ri/Sqrt(A)	2.26	4.09
ATTENUATION DETAILS:			
TESCH	Tesch leg atten	3.09E-01	8.09E-03
	Tesch vent attenuation:		2.50E-03
	Angle, source to leg 1 axis (deg)		0
	Source Geometry Effect		0.250
	Total Tesch Vent Attenuation		6.24E-04
GOEBEL	Goebel leg atten	6.89E-02	5.56E-03
	Total Goebel Vent Attenuation		3.83E-04
MEAN	Geometric Mean Vent Attenuation		4.89E-04
	"Variance" factor:		1.28

SOURCE TERM:		
	No. of ions lost	1.14E+11
	Std star per cc/ion lost	1.35E-04
	Dose-Equiv (rem) per star	2.66E-05
	Low Energy Fraction	0.85
	Entrance Dose-Equiv (rem)	2.44E+02
OVERALL RESULT:		
	Exit Dose (rem) [Tesch]	1.52E-01
	Exit Dose (rem) [Goebel]	9.34E-02
	Geometric Mean	*1.19E-01*

RHIC EMERGENCY EXHAUST DUCTS, archetype results

	Vent Case	**F-2**
	Location	INJ-EJECT AT SEXT 5,7
	Geometry Comments	Far Wall

		Leg 1	Leg 2
GEOMETRY	**DATA:**		
INPUT	dist to Beam (ft)	14.25	
	pipe dia (in)	48.00	
	horiz. pipe length, d1 (ft)	6.00	
	vertical CL length, d2 (ft)		16.50
METRIC	distance to beam, a (m)	4.34	
	horiz. pipe length, d1 (m)	1.83	
	vertical CL pipe length, d2 (m)		5.03
	pipe dia (m)	1.22	1.22
	pipe area, A (sq m)	1.17	1.17
LEG LENGTHS (meters):			
	Leg 1 length to mid-bend, R1 (m)	2.44	
TESCH	Leg 1: Source to mid-bend, r1 = R1 + a	6.78	
TESCH	Leg 2, length from leg 1 pipe, R2		4.42
GOEBEL	Leg length, Ri/Sqrt(A)	2.26	4.09
ATTENUATION DETAILS:			
TESCH	Tesch leg atten	4.10E-01	8.09E-03
	Tesch vent attenuation:		3.32E-03
	Angle, source to leg 1 axis (deg)		0
	Source Geometry Effect		0.250
	Total Tesch Vent Attenuation		8.30E-04
GOEBEL	Goebel leg atten	6.89E-02	5.56E-03
	Total Goebel Vent Attenuation		3.83E-04
MEAN	Geometric Mean Vent Attenuation		5.64E-04
	"Variance" factor:		1.47

SOURCE TERM:		
	No. of ions lost	1.14E+11
	Std star per cc/ion lost	1.35E-04
	Dose-Equiv (rem) per star	2.66E-05
	Low Energy Fraction	0.85
	Entrance Dose-Equiv (rem)	1.20E+02
OVERALL RESULT:		
	Exit Dose (rem) [Tesch]	9.97E-02
	Exit Dose (rem) [Goebel]	4.60E-02
	Geometric Mean	6.77E-02

RHIC EMERGENCY EXHAUST DUCTS, archetype results

Vent Case	**G-1**	
Location	INJ/EJCTS AT WIDE ANGLE	
Geometry Comments	Near Wall	

		Leg 1	Leg 2
GEOMETRY	**DATA:**		
INPUT	dist to Beam (ft)	8.25	
	pipe dia (in)	48.00	
	horiz. pipe length, d1 (ft)	6.00	
	vertical CL length, d2 (ft)		16.50
METRIC	distance to beam, a (m)	2.51	
	horiz. pipe length, d1 (m)	1.83	
	vertical CL pipe length, d2 (m)		5.03
	pipe dia (m)	1.22	1.22
	pipe area, A (sq m)	1.17	1.17
LEG LENGTHS (meters):			
	Leg 1 length to mid-bend, R1 (m)	2.44	
TESCH	Leg 1: Source to mid-bend, r1 = R1 + a	4.95	
TESCH	Leg 2, length from leg 1 pipe, R2		4.42
GOEBEL	Leg length, Ri/Sqrt(A)	2.26	4.09
ATTENUATION DETAILS:			
TESCH	Tesch leg atten	2.58E-01	8.09E-03
	Tesch vent attenuation:		2.09E-03
	Angle, source to leg 1 axis (deg)		0
	Source Geometry Effect		0.250
	Total Tesch Vent Attenuation		5.21E-04
GOEBEL	Goebel leg atten	6.89E-02	5.58E-03
	Total Goebel Vent Attenuation		3.83E-04
MEAN	Geometric Mean Vent Attenuation		4.47E-04
	"Variance" factor:		1.17
SOURCE TERM:			
	No. of ions lost		1.14E+11
	Std star per cc/ion lost		1.35E-04
	Dose-Equiv (rem) per star		2.66E-05
	Low Energy Fraction		0.85
	Entrance Dose-Equiv (rem)		3.58E+02
OVERALL RESULT:			
	Exit Dose (rem) [Tesch]		1.87E-01
	Exit Dose (rem) [Goebel]		1.37E-01
	Geometric Mean		*1.60E-01*

RHIC EMERGENCY EXHAUST DUCTS, archetype results

Vent Case	**G-2**	
Location	INJ/EJCTS AT WIDE ANGLE	
Geometry Comments	Far Wall	

		Leg 1	Leg 2
GEOMETRY	**DATA:**		
INPUT	dist to Beam (ft)	10.00	
	pipe dia (in)	48.00	
	horiz. pipe length, d1 (ft)	6.00	
	vertical CL length, d2 (ft)		16.50
METRIC	distance to beam, a (m)	3.05	
	horiz. pipe length, d1 (m)	1.83	
	vertical CL pipe length, d2 (m)		5.03
	pipe dia (m)	1.22	1.22
	pipe area, A (sq m)	1.17	1.17
LEG LENGTHS (meters):			
	Leg 1 length to mid-bend, R1 (m)	2.44	
TESCH	Leg 1: Source to mid-bend, r1 = R1 + a	5.49	
TESCH	Leg 2, length from leg 1 pipe, R2		4.42
GOEBEL	Leg length, Ri/Sqrt(A)	2.26	4.09
ATTENUATION DETAILS:			
TESCH	Tesch leg atten	3.09E-01	8.09E-03
	Tesch vent attenuation:		2.50E-03
	Angle, source to leg 1 axis (deg)		0
	Source Geometry Effect		0.250
	Total Tesch Vent Attenuation		6.24E-04
GOEBEL	Goebel leg atten	6.89E-02	5.56E-03
	Total Goebel Vent Attenuation		3.83E-04
MEAN	Geometric Mean Vent Attenuation		4.89E-04
	"Variance" factor:		1.28
SOURCE TERM:			
	No. of ions lost		1.14E+11
	Std star per cc/ion lost		1.35E-04
	Dose-Equiv (rem) per star		2.66E-05
	Low Energy Fraction		0.85
	Entrance Dose-Equiv (rem)		2.44E+02
OVERALL RESULT:			
	Exit Dose (rem) [Tesch]		1.52E-01
	Exit Dose (rem) [Goebel]		9.34E-02
	Geometric Mean		*1.19E-01*

RHIC EMERGENCY EXHAUST DUCTS, archetype results

Vent Case	**H**	
Location	RF CAVITY SEXT. 5	
Geometry Comments		

		Leg 1	Leg 2
GEOMETRY DATA:			
INPUT	dist to Beam (ft)	10.00	
	pipe dia (in)	42.00	
	horiz. pipe length, d1 (ft)	6.00	
	vertical CL length, d2 (ft)		17.50
METRIC	distance to beam, a (m)	3.05	
	horiz. pipe length, d1 (m)	1.83	
	vertical CL pipe length, d2 (m)		5.33
	pipe dia (m)	1.07	1.07
	pipe area, A (sq m)	0.89	0.89
LEG LENGTHS (meters):			
	Leg 1 length to mid-bend, R1 (m)	2.36	
TESCH	Leg 1: Source to mid-bend, r1 = R1 + a	5.41	
TESCH	Leg 2, length from leg 1 pipe, R2		4.80
GOEBEL	Leg length, Ri/Sqrt(A)	2.50	5.08
ATTENUATION DETAILS:			
TESCH	Tesch leg atten	3.17E-01	4.88E-03
	Tesch vent attenuation:		1.55E-03
	Angle, source to leg 1 axis (deg)		0
	Source Geometry Effect		0.250
	Total Tesch Vent Attenuation		3.87E-04
GOEBEL	Goebel leg atten	5.53E-02	2.88E-03
	Total Goebel Vent Attenuation		1.59E-04
MEAN	Geometric Mean Vent Attenuation		2.48E-04
	"Variance" factor:		1.56

SOURCE TERM:		
	No. of ions lost	1.14E+11
	Std star per cc/ion lost	1.35E-04
	Dose-Equiv (rem) per star	2.66E-05
	Low Energy Fraction	0.85
	Entrance Dose-Equiv (rem)	2.44E+02
OVERALL RESULT:		
	Exit Dose (rem) [Tesch]	9.45E-02
	Exit Dose (rem) [Goebel]	3.88E-02
	Geometric Mean	*6.05E-02*

RHIC EMERGENCY EXHAUST DUCTS, archetype results

	Vent Case	**I-1**	
	Location	ALCOVE A AND C - TYPICAL	
	Geometry Comments		
GEOMETRY	**DATA:**	**Leg 1**	**Leg 2**
INPUT	dist to Beam (ft)	15.50	
	pipe dia (in)	42.00	
	horiz. pipe length, d1 (ft)	6.00	
	vertical CL length, d2 (ft)		10.00
METRIC	distance to beam, a (m)	4.72	
	horiz. pipe length, d1 (m)	1.83	
	vertical CL pipe length, d2 (m)		3.05
	pipe dia (m)	1.07	1.07
	pipe area, A (sq m)	0.89	0.89
LEG LENGTHS (meters):			
	Leg 1 length to mid-bend, R1 (m)	2.36	
TESCH	Leg 1: Source to mid-bend, r1 = R1 + a	7.09	
TESCH	Leg 2, length from leg 1 pipe, R2		2.51
GOEBEL	Leg length, Ri/Sqrt(A)	2.50	2.66
ATTENUATION DETAILS:			
TESCH	Tesch leg atten	4.44E-01	2.01E-02
	Tesch vent attenuation:		8.95E-03
	Angle, source to leg 1 axis (deg)		15
	Source Geometry Effect		0.250
	Total Tesch Vent Attenuation		2.24E-03
GOEBEL	Goebel leg atten	5.53E-02	1.61E-02
	Total Goebel Vent Attenuation		8.92E-04
MEAN	Geometric Mean Vent Attenuation		1.41E-03
	"Variance" factor:		1.58
SOURCE TERM:			
	No. of ions lost		1.14E+11
	Std star per cc/ion lost		1.35E-04
	Dose-Equiv (rem) per star		2.66E-05
	Low Energy Fraction		0.85
	Entrance Dose-Equiv (rem)		1.02E+02
OVERALL RESULT:			
	Exit Dose (rem) [Tesch]		2.27E-01
	Exit Dose (rem) [Goebel]		9.06E-02
	Geometric Mean		*1.43E-01*

RHIC EMERGENCY EXHAUST DUCTS, archetype results

	Vent Case	**I-2**
	Location	ALCOVE A AND C - TYPICAL
	Geometry Comments	

		Leg 1	Leg 2
GEOMETRY	**DATA:**		
INPUT	dist to Beam (ft)	15.50	
	pipe dia (in)	48.00	
	horiz. pipe length, d1 (ft)	6.00	
	vertical CL length, d2 (ft)		10.00
METRIC	distance to beam, a (m)	4.72	
	horiz. pipe length, d1 (m)	1.83	
	vertical CL pipe length, d2 (m)		3.05
	pipe dia (m)	1.22	1.22
	pipe area, A (sq m)	1.17	1.17
LEG LENGTHS (meters):			
	Leg 1 length to mid-bend, R1 (m)	2.44	
TESCH	Leg 1: Source to mid-bend, r1 = R1 + a	7.16	
TESCH	Leg 2, length from leg 1 pipe, R2		2.44
GOEBEL	Leg length, Rl/Sqrt(A)	2.26	2.26
ATTENUATION DETAILS:			
TESCH	Tesch leg atten	4.35E-01	2.72E-02
	Tesch vent attenuation:		1.18E-02
	Angle, source to leg 1 axis (deg)		15
	Source Geometry Effect		0.250
	Total Tesch Vent Attenuation		2.96E-03
GOEBEL	Goebel leg atten	6.89E-02	2.27E-02
	Total Goebel Vent Attenuation		1.56E-03
MEAN	Geometric Mean Vent Attenuation		2.15E-03
	"Variance" factor:		1.38
SOURCE TERM:			
	No. of ions lost		1.14E+11
	Std star per cc/ion lost		1.35E-04
	Dose-Equiv (rem) per star		2.66E-05
	Low Energy Fraction		0.85
	Entrance Dose-Equiv (rem)		1.02E+02
OVERALL RESULT:			
	Exit Dose (rem) [Tesch]		3.00E-01
	Exit Dose (rem) [Goebel]		1.58E-01
	Geometric Mean		*2.18E-01*

RHIC EMERGENCY EXHAUST DUCTS, archetype results

Vent Case	**J-1**	
Location	ALCOVE B - TYPICAL	
Geometry Comments		

		Leg 1	Leg 2
GEOMETRY	**DATA:**		
INPUT	dist to Beam (ft)	16.00	
	pipe dia (in)	42.00	
	horiz. pipe length, d1 (ft)	6.00	
	vertical CL length, d2 (ft)		13.00
METRIC	distance to beam, a (m)	4.88	
	horiz. pipe length, d1 (m)	1.83	
	vertical CL pipe length, d2 (m)		3.96
	pipe dia (m)	1.07	1.07
	pipe area, A (sq m)	0.89	0.89
LEG LENGTHS (meters):			
	Leg 1 length to mid-bend, R1 (m)	2.36	
TESCH	Leg 1: Source to mid-bend, r1 = R1 + a	7.24	
TESCH	Leg 2, length from leg 1 pipe, R2		3.43
GOEBEL	Leg length, Ri/Sqrt(A)	2.50	3.63
ATTENUATION DETAILS:			
TESCH	Tesch leg atten	4.54E-01	9.63E-03
	Tesch vent attenuation:		4.37E-03
	Angle, source to leg 1 axis (deg)		50
	Source Geometry Effect		0.100
	Total Tesch Vent Attenuation		4.37E-04
GOEBEL	Goebel leg atten	5.53E-02	7.72E-03
	Total Goebel Vent Attenuation		4.26E-04
MEAN	Geometric Mean Vent Attenuation		4.32E-04
	"Variance" factor:		1.01
SOURCE TERM:			
	No. of ions lost		1.14E+11
	Std star per cc/ion lost		1.35E-04
	Dose-Equiv (rem) per star		2.66E-05
	Low Energy Fraction		0.85
	Entrance Dose-Equiv (rem)		9.53E+01
OVERALL RESULT:			
	Exit Dose (rem) [Tesch]		4.16E-02
	Exit Dose (rem) [Goebel]		4.06E-02
	Geometric Mean		*4.11E-02*

RHIC EMERGENCY EXHAUST DUCTS, archetype results

Vent Case	**J-2**	
Location	ALCOVE B - TYPICAL	
Geometry Comments		

		Leg 1	Leg 2
GEOMETRY DATA:			
INPUT	dist to Beam (ft)	16.00	
	pipe dia (in)	48.00	
	horiz. pipe length, d1 (ft)	6.00	
	vertical CL length, d2 (ft)		13.00
METRIC	distance to beam, a (m)	4.88	
	horiz. pipe length, d1 (m)	1.83	
	vertical CL pipe length, d2 (m)		3.96
	pipe dia (m)	1.22	1.22
	pipe area, A (sq m)	1.17	1.17
LEG LENGTHS (meters):			
	Leg 1 length to mid-bend, R1 (m)	2.44	
TESCH	Leg 1: Source to mid-bend, r1 = R1 + a	7.32	
TESCH	Leg 2, length from leg 1 pipe, R2		3.35
GOEBEL	Leg length, Ri/Sqrt(A)	2.26	3.10
ATTENUATION DETAILS:			
TESCH	Tesch leg atten	4.44E-01	1.37E-02
	Tesch vent attenuation:		6.09E-03
	Angle, source to leg 1 axis (deg)		50
	Source Geometry Effect		0.100
	Total Tesch Vent Attenuation		6.09E-04
GOEBEL	Goebel leg atten	6.89E-02	1.14E-02
	Total Goebel Vent Attenuation		7.84E-04
MEAN	Geometric Mean Vent Attenuation		6.91E-04
	"Variance" factor:		1.13

SOURCE TERM:		
	No. of ions lost	1.14E+11
	Std star per cc/ion lost	1.35E-04
	Dose-Equiv (rem) per star	2.66E-05
	Low Energy Fraction	0.85
	Entrance Dose-Equiv (rem)	9.53E+01
OVERALL RESULT:		
	Exit Dose (rem) [Tesch]	5.80E-02
	Exit Dose (rem) [Goebel]	7.47E-02
	Geometric Mean	*6.58E-02*

AD/RHIC/RD–76

RHIC PROJECT

Brookhaven National Laboratory

Shielding of Multi-Leg Penetrations into the RHIC Collider

Peter J. Gollon

October 1994

SHIELDING OF MULTI-LEG PENETRATIONS INTO THE RHIC COLLIDER

Peter J. Gollon

May 23, 1994

I. INTRODUCTION:

This report documents the neutron leakage calculations done for the multi-leg penetrations leading into the RHIC Injection Line and Collider tunnels. These penetrations are labyrinths for personnel and equipment access, or air ducts for emergency ventilation. With the exception of the new structures at the 10 and 12 o'clock areas, the tunnel penetrations were designed for the much higher beam energies and currents of the former CBA project, so no problems were anticipated when the lower intensity heavy ion accelerator RHIC was placed in the tunnel. However, it appeared prudent to recalculate the attenuation and neutron dose equivalent outside the as-built penetrations at the same time that the labyrinths for the newly designed 10 and 12 o'clock regions were being calculated.

The facilities covered by this report are shown in Figure 1. In particular, this report includes the transfer tunnel from the AGS, the curved RHIC ring tunnels, and all intersection regions. Calculated results are given for neutron dose attenuation of all the personnel access labyrinths and air vents. Combining this calculated dose attenuation with standard beam loss assumptions yields the additional dose outside these tunnels resulting from the presence of these penetrations. Although within the geographical scope of the RHIC Project, this report does not address any straight penetrations, i.e. those in which the tunnel can be viewed directly from the outside, since they require different calculational techniques and approximations. Examples of such straight penetrations are the cryogenic "chimneys" next to each experimental area, the survey holes around the ring, and the cable ducts which will be filled to an as yet unknown degree with shielding material in the form of polyethylene and copper cable.

II. DESCRIPTION OF THE CALCULATION:

The dose (or dose equivalent) in the vicinity of a penetration in a hadron shield may be thought of as consisting of three parts. The first component is the dose which would be present in the absence of any penetration. In the present situation, this is determined by the propagation of the hadron cascade from the loss point through the hadron shield to the outside world. There are a variety of methods for calculating this, with Monte Carlo methods currently being preferred over analytic approximations for all but the simplest situations.

The second component may be thought of as the additional radiation propagating through the shield as a result of the shield's being weakened by the removal of material to make the penetration. This additional radiation passes through a hadron shield of reduced thickness, but is otherwise similar in spectral quality to the radiation passing through the full thickness of the shield. This component is discussed at length by Stevens [ST-94]..For all the 3-legged labyrinths, estimates

are made here of the additional low energy neutron dose ("punch-through") caused by the hadron cascade short-circuiting the first two legs of the labyrinth..

The third component is the radiation which passes through the penetration itself, with only minimal interaction in the bulk shield. In the case of a straight penetration into the accelerator enclosure, this component could include secondary and later generation particles originating in hadron cascades in the accelerator components or facing walls. Because they do not come from an equilibrium spectrum, these particles would have their average energies well above those which pass through the thick hadron shield.

In the case of a multi-legged labyrinth the high energy particles characteristic of the hadron cascade do not get past the first bend of the labyrinth. Those particles that do get past the bends in a labyrinth, and thus carry most of the dose equivalent, are neutrons with energies between thermal and a few MeV. The spectrum of neutrons propagating down a labyrinth softens with increasing distance from the source, and is softer for a softer neutron source. Vogt [VO-75] has some particularly clear calculational results on this subject. Because of the different energy spectra of the particles carrying the dose equivalent in the case of straight and multi-leg penetrations, different approximations are necessary for these two situations. The present work deals primarily with the third component, i.e., the low energy neutrons emerging from a multi-legged labyrinth.

The first step in the calculation is the choice of a beam loss scenario: how many high energy protons or ions will be lost at a particular location, and what hadron flux will that loss produce at the tunnel wall where the labyrinth enters the RHIC enclosure. This beam loss scenario sets the scale for the calculations: if more or fewer particles are actually lost, then the resulting dose equivalents will be proportionately higher or lower.

The second step is the calculation of the attenuation of the dose equivalent in the labyrinth itself, both as a result of simply moving further away from regions of higher flux, and as a result of turning a corner. The attenuation of radiation as it propagates through the labyrinth depends not only on the labyrinth design *per se*, but also on the position of the labyrinth in relation to the beam loss point or RHIC magnet.

Finally, for each three-legged labyrinth considered I have made a rough estimate of the extra high energy dose equivalent resulting from a weakening of the shield caused by the presence of the labyrinth. The mechanism considered is that the radially propagating high energy cascade short circuits the first two legs by "punching through" the shield to the bend between the second and third legs, and then produces evaporation neutrons which diffuse out of the third leg unimpeded.

III. BEAM LOSS SCENARIOS:

RHIC is a complex of two counter-rotating intersecting heavy ion accelerator-storage rings in the same underground tunnel. Each ring will be filled in turn from the existing Alternate Gradient Synchrotron (AGS) via a transfer line and injection system. The beam particles could range from protons to gold ions. The day-one operating scenario outlined in the Conceptual Design Report uses 57 AGS bunches to fill each RHIC ring, each bunch having either 1×10^9 Au ions, or 1×10^{11}

protons. A RHIC ring will be filled by AGS pulses consisting of either 3 bunches of heavy ions at 10.4 GeV/u with a 1.5 second cycle time, or 12 bunches of protons at 28 GeV/u every 2 seconds. A stacked current four times higher is assumed here for calculational purposes; this is assumed to be achieved using twice as many AGS bunches, each with twice the number of particles given in the Design Manual. Thus the stored current in each RHIC ring will be taken as either 2.28×10^{11} Au ions, or 2.28×10^{13} protons.

The stored beam will be accelerated to experimental energy (typically between a few times the injection energy and 250 GeV/u for protons or 100 GeV/u for gold) and stored for a period of hours [BNL-89]. When the beam quality deteriorates sufficiently to hamper the experiments by reducing the interaction rate or raising the background rate, it will be dumped in special-purpose beam dumps, and the injection, storage and acceleration cycle will start anew. However, the losses during routine operation will be minimal, and it is shown by Harrison and Stevens [HA-92] that large losses in the Collider during a possible fault, rather than the low chronic losses, are the limiting factor for personnel exposure.

There are a number of different beam loss scenarios which have been considered separately:

Transfer Line Fault Losses: It is the intention of the RHIC Project to provide interlocked radiation monitors at appropriate locations outside the shielding to inhibit further AGS operation if large transfer line losses occur on two successive AGS pulses. [ST-92] Because each AGS proton pulse has four times the number of bunches as a heavy ion pulse, more radiation is produced *per pulse* for protons under fault conditions involving the loss of an entire pulse in the Transfer Line. Thus the source term used here for the transfer line consists of losses which occur during two AGS pulses of 2.4×10^{12} protons at 28 GeV/c.

Chronic Transfer Line Losses: The various routine beam losses in the transfer line are discussed by Harrison and Stevens [HA-92]. In particular, the largest routine operational loss was taken to be 0.05% of the beam on any magnet in the Transfer Line. When the loss of the same fraction of the Au and proton beams are compared, the Au ions produce more radiation than do the protons. When the operating cycle of RHIC is factored in, the case producing the highest dose rates is the loss of 8.28×10^{8} Au ions per hour, or 8.78×10^{11} Au ions per year [ST-92]. If the largest chronic loss of 0.05% occurred at the same location for a full year's operation of the Transfer Line, the resulting dose outside the shielding would be about 18 times greater than that resulting from the loss of two pulses of 2.4×10^{12} protons at 28 GeV/c. Both the Transfer Line chronic losses and fault losses need to be considered separately.

RHIC Tunnel Beam Losses: Beam losses can range from routine and expected but low operating losses, to the extremely large loss of a major fraction of the accelerator intensity during a fault condition. All calculations here assume an intensity of four times the Design Manual beam intensity, that is, 2.28×10^{11} Au ions per beam. The highest anticipated stored beam energy (100 GeV/u) for heavy ions was used for losses inside the RHIC tunnel. Because of the extremely clean nature of the stored RHIC beam, the dose from the chronic losses will be negligible compared to the possible dose from a fault.

We make the reasonable assumption that a large uncontrolled beam loss (fault condition) would involve the beam in only one ring. Although it is easy to conceive of an entire beam being lost, it is not possible to define a sequence of events which would realistically lead to an uncontrolled loss of 100% of the beam at a single point. We thus follow Harrison and Stevens [HA-92] in assuming that the most serious but still realistic failure scenario ("maximum credible fault") involves the loss or scraping of not more than 50% of one beam at an arbitrary location (i.e. a magnet), with the remainder of the loss being distributed around the ring. They consider faults involving the loss of an entire beam at one point to be possible only at aperture-defining locations such as high-beta quadrupoles, limiting aperture collimators and the beam dump. So long as aperture defining objects are not placed near penetrations into the RHIC tunnel, it is not necessary for purposes of this calculation to consider the loss of 100% of the stored beam at a single point. Calculations by Stevens again indicate that loss of the Au beam is more effective than the loss of the proton beam in producing secondary radiation, so we consider only that case here.

RHIC Experimental Hall Beam Losses: The approach discussed above makes sense when applied to a magnet enclosure, within which the size and location of the magnets and other large objects are known. It does not make sense to use this approach with the experimental halls, since it is not useful to calculate a "worst case" situation with an otherwise empty hall. The empty halls have thinly shielded areas such as their roofs and front walls. The apparatus that goes inside a hall will be massive enough to provide significant shielding against losses. One attempt to calculate the self-shielding of a RHIC detector has been made by A. J. Stevens for the STAR detector. [ST-92b] This self-shielding must be considered when calculating dose rates outside the shield, whether that dose occurs as a result of radiation penetrating the thin shield, or escaping through openings in it. The appropriate standard for the attenuation of a multi-leg penetration in an experimental hall is that the labyrinth provide better attenuation than the nearby fixed shielding. For then the addition of enough additional shielding or apparatus inside the hall to make the radiation levels outside the shield acceptably low, will also make the levels outside the penetration acceptably low. Of course, the definition of an "acceptably low" level depends on the accessibility and occupation of the area; and the thinly shielded experimental hall roofs will be fenced if the anticipated radiation levels there require it.

In light of the preceeding discussion, although the nominal dose rate at the opening of each vent in an experimental hall is calculated using an unrealistic empty hall assumption, and the dose-equivalent attenuation of each duct is estimated, these two numbers are *not* multiplied together to "predict" what the DE rate outside the duct would be in the event of a beam loss inside the hall.

IV. MONTE CARLO CALCULATION OF SOURCE TERM:

The dose rate outside a penetration can be calculated as the product of the dose rate incident on the mouth of the penetration in the magnet enclosure, multiplied by the neutron attenuation of the penetration itself. The hadron Monte Carlo cascade program CASIM [VAN-75], as modified and updated by Alan Stevens, [ST-90] was used by Stevens to determine the dose striking the tunnel wall at the location of each labyrinth mouth.

For losses in the Transfer line, we use the "sparse lattice" calculations for 10.4 GeV/u Au ions and 28 Gev protons reported by Stevens in ST-92. That calculation considers the loss of the

transported beam inside a magnet within a magnet enclosure of radius 1.5 meters. The secondary and subsequent generation particles are transported through the magnet and into the earth tunnel walls. Results for the maximum star density as a function of radial shielding thickness are shown in that reference as Figures 2 and 3.

Stevens computed two different cases for losses inside the RHIC Collider. The first case assumed the beam scraped on the beampipe of RHIC quadrupole Q1. The second case assumed the scraping occurred on a quadrupole in the regular lattice. In both cases, he then propagated the lost beam and secondary radiation through the downstream magnets inside a typical RHIC magnet enclosure of radius 2.5 meters. [A. J. Stevens, private communication]. Both calculations gave essentially identical results for the maximum star density at the tunnel walls (1.35×10^{-4} star/cm^3 in soil per ion lost). Plots of the star density in the tunnel wall as a function of distance from the loss point are shown in Figure 2. None of the labyrinths entered tunnels whose radius exactly matched the 2.5 m radius assumed in the Monte Carlo cascade calculations, so the calculated star density was scaled to the appropriate tunnel radius using inverse square scaling.

The result of a CASIM calculation is the star density for hadrons with energies above a particular threshold, usually 300 Mev/c, equivalent to 49 Mev for nucleons. This star density must be converted to dose equivalent to be useful here. Following Stevens [ST-92], we use Van Ginneken's original star to dose conversion factor, rather than the lower one proposed by Stevenson [ST-88]. Van Ginneken's conversion factor of 9.0×10^{-6} rem/star in concrete (density = 2.3 gm/cm^3) can be generalized as:

$$\text{Dose-equiv (rem)} = 2.25 \times 10^{-7} \times L \times (\text{stars/cm}^3), \qquad (1)$$

where L is the high energy neutron interaction length in cm. For BNL soil (density = 1.8), L = 53.3 cm. This conversion factor is then modified by an additional factor of two in anticipation of a doubling of the quality factors for low energy neutrons, as given in the new facility design criteria in the "RadCon" Manual [DOE-92].

However, not all of the radiaton incident on the mouth of a labyrinth is equally well propagated through the first leg of that labyrinth. Some of the dose equivalent inside the magnet enclosure is due to high energy hadrons propagating in a generally forward direction, down the magnet enclosure. Those high energy hadrons which do enter the labyrinth at a such a shallow angle will bury themselves in the downstream labyrinth wall, rather than propagate in a direction nearly perpendicular to the beam. Thus the high energy part of the spectrum contributes minimally to the leakage through the labyrinth. In contrast to this, the lower energy neutrons which emerge from the magnets or nearby walls have an approximately isotropic distribution. Thus they can freely propagate down the first leg of any penetration that "looks" at the beamline. Vogt [VO-75] suggests 20 MeV as the energy above which "neutrons may be neglected if the source cannot be seen from the point of detection.... This effect is due to the ratio of elastic and total cross-section involving a decreasing albedo with increasing energy in this range." Vogt's calculations, using the analog Monte Carlo program SAM-CE, indicate that the exact spectral shape of the incident spectrum is not critical to the dose attenuation, and that neutrons of all energies below this suggested maximum have approximately the same attenuation.

To determine the fraction of incident dose equivalent carried by neutrons of energy less than 20 MeV, we need to know the incident neutron spectrum. For a spectrum characteristic of a fully developed hadron cascade in soil or concrete, Figs. VI.12 and VI.13 of Van Ginneken and Awschalom [VA-75] suggest that 65% of the dose equivalent is carried by neutrons below 20 MeV. Of course, the spectrum outside a RHIC magnet is far from an equilibrium spectrum, and would thus be expected to be harder than an equilibrium spectrum. The corresponding results for a much harder spectrum outside a 5 cm radius iron target may be obtained from Fig. VI.8 as 15%. This figure is an underestimate for two reasons: the RHIC magnets are thicker than a mere 5 cm, and Van Ginneken and Awschalom ignored the "hole" in the iron non-elastic cross section below about 1 MeV. This effect is taken into acount by Gollon [GO-76] for an iron magnet of 28 cm radius. Figure 3 of this reference indicates that fully 85% of the dose equivalent is carried by neutrons of energy less than 20 MeV. This latter figure will be used in the subsequent calculations. Use of softer this spectrum also results in a slightly higher flux-to-dose conversion factor of 10.2×10^{-6} rem/star in concrete [GO-76], or more generally:

$$\text{Dose-equiv (rem)} = 2.5 \times 10^{-7} \times L \times (\text{stars/cm}^3), \qquad (1a)$$

V. LABYRINTH CALCULATONS:

Straight-Legged Labyrinths:

A number of different techniques exist for the calculation of neutron leakage through access labyrinths. Brief reviews of the different calculational techniques, including analog and albedo Monte Carlo methods, are given by Routti and Van de Voorde [RO-75], by Vogt [VO-75], and by Stevenson [ST-87b]. (An "albedo" Monte Carlo program treats the neutrons as if they were reflected from the *surface* of the material they strike, instead of following their actual behavior as they enter the enclosure wall, multiple scatter, and then perhaps emerge some distance from their entry point. The "analog" Monte Carlo programs attempt to reproduce these detailed neutron interactions in the enclosure walls; as a result they execute much more slowly than the albedo programs.) These articles should be consulted by those interested in a detailed discussion of the subject.

Ultimately all calculational techniques are based on labyrinth measurements, or are validated by comparison with such measurements. Unfortunately, the geometries and other conditions on which they are based, or with which they are validated, are not mutually compatible, nor are they entirely compatible with the conditions here. Further, the predictions made by the various techniques when applied to the same geometry do not agree as closely as one would like.

A key feature in all calculations is the attenuation of the transmitted dose down the first leg, since this depends strongly on the position of the source in relation to the opening of the first leg. Low energy measurements by Tesch and high energy measurements by Cossairt et. al both indicate that the actual first leg falloff is somewhat *faster* than $1/r^2$ for an *on*-axis source. The origin of this deviation is thought to be those neutrons which scatter in the accelerator enclosure and enter the labyrinth with an off-axis direction, striking a wall some distance down the first leg. By thus contributing to the dose at the front of the leg, but not at the back, they produce a falloff faster than inverse square.

When the source extends beyond the opening of the labyrinth, or is located off the axis of the first leg, the attenuation of the first leg is considerably better than for a point source on-axis. This is a result of the small number of neutrons which enter the first leg more or less parallel to its axis and thus propagate to the end of that leg withour first striking a wall. The different calculational techniques reproduce these effects much more unevenly than they do for a source on the axis of the first leg, or for a second leg.

For example, one of the easiest techniques to use prior to the advent of personal computers was the graphical scaling of Gollon and Awschalom [GO-71] based on their Monte Carlo calculations using the monokinetic (single energy group) albedo Monte Carlo code ZEUS [GE-68]. The experimental measurements of dose attenuation reported by Cossairt et al. [CO-85] and shown in Figure 4 match the scaled curves of Gollon and Awschalom, as well as the formulas of Tesch (see below). The agreement between measurement and both calculational techniques is best in the first two legs of his multi-leg experiment; in the third leg both techniques underestimate the measured dose by a factor of about three. This underestimate may be caused by neutron punch-through which short-circuits the first two legs of the labyrinth being measured. However, this discrepancy may also be caused by the tendency of these techniques to underestimate the transmitted dose at deep depths in multi-leg labyrinths. This is shown by their comparison with the presumably more accurate analog Monte Carlo programs MORSE and SAM-CE quoted by Stevenson [ST-82b] and by Goebel et al. [GO-75]. In addition, the first leg"point source off-axis" flux of Gollon and Awschalom in particular is quite likely very much too low.

Both the ZEUS and SAM-CE results have the advantage of scaling: all dimensions are measured in terms of the square root of the cross sectional area of the duct. When dimensions are given in this way, all ducts of similar shapes but whose physical dimensions differ by a constant multiple have the same dose attenuation curves. (This simplificaton generally works for height:width ratios between 1:1 and 2:1.) This greatly facilitates calculations and comparisons between different ducts. In practice one has to be make sure that the source geometry scales appropriately before using such curves for the first leg.

The SAM-CE results discussed by Goebel et al. have their own difficulties. The source geometry used for the various calculations is never fully described, so it is unclear how to adapt the given results to a modified geometry. Further, their various SAM-CE calculations are not consistent: some of their graphs show point sources having faster attenuation with distance down the labyrinth than line sources which extend past the labyrinth mouth. On simple geometric grounds, this is not possible.

Goebel et al. reduce the effects of the difficulties of the ZEUS and SAM-CE calculations by combining the results of these calculations with various measurements to yield a set of "universal curves" for the first leg (point source on axis, line source, point source off axis or plane source), and a single curve for the second leg. These curves give the dose H(d) at any point down a labyrinth leg in terms of the dose H(0) at the entrance to that leg and the distance d measured from the beginning of the leg in units of the square root of the cross sectional area of that leg. Stevenson and Fassò [ST-87c] parameterize the curve for the first leg dose from a plane source or point source off axis as:

$$H(d) = H(0)/(1 + 2.5\sqrt{d} + 0.17d^{1.7} + 0.79d^{3}) \qquad (2)$$

and the second leg dose as:

$$H(d) = H(0)/(1 + 2.8\, d\, (1.57)^{d+2}) \qquad (3)$$

They also compare dose attenuation measurements in a 1 meter diameter shaft going down to the CERN SPS tunnel with predictions based on Goebel's "universal curves". Goebel's "universal curves" provided one method for evaluating the RHIC duct attenuations.

For a second, independent method I chose the empirical formulas of Tesch [TE-82]. These are based on the measured attenuation of ^{252}Cf fission and ^{241}Am-Be neutron sources in a labyrinth built of concrete blocks. Tesch's original formula for the dose equivalent in the first leg is a modified inverse-square dependence suitable for a penetration which directly views a point neutron source:

$$H(r_1) = 2\, H_0(a) a^2 r_1^{-2} \qquad (4)$$

Here $H(r_1)$ is the dose equivalent rate as a function of distance r_1 down the first leg, as measured from the point source, and a is the distance from the source (beam line) to the mouth of the first leg. (There is no uniform notation for these distances in the literature, although this notation is consistent with that of Tesch and of Cossairt.) H_0 is the dose calculated to exist a distance a away from the source in the absence of scattering by the accelerator enclosure. This notation is shown in Figure 5, which represents a typical 3-legged personnel access labyrinth. A typical 2-legged ventilation duct is shown with its associated notation as Figure 6.

The factor of two in Equation (4) takes into account those neutrons which leave the point source heading away from the labyrinth, but which are scattered into the labyrinth opening by one of the walls of the accelerator enclosure. The extra factor of two is appropriate when the calculated flux at the labyrinth opening is based on an inverse square model which includes only neutrons going directly from the neutron source to the labyrinth opening. This is not so in the present case. The calculated star density at the wall includes neutrons coming from interactions in the tunnel walls and from interactions in the magnet. Since the CASIM conversion factor from star density to dose equivalent of Equation (1) incorporates the omni-directional low energy neutrons that would come from backscattering from the accelerator enclosure wall, this empirical correction factor of two is not necessary. The low energy neutron spectrum used in GO-76 was taken from calculations by Armstrong and Alsmiller [AR-69] using an analog Monte Carlo technique that included neutron backscatter, so no correction is necessary if Equation (1a) is used, either.

For the second and subsequent legs, Tesch presents a formula which is the sum of two exponentials:

$$H(r_k) = H(0)\, \frac{c_k[\exp(-r_k/0.45) + 0.022\, A_k^{1.3} \exp(-r_k/2.35)]}{[1 + 0.022\, A_k^{1.3}]} \qquad (5)$$

Here A_k is the cross sectional area of the enclosure in square meters, and r_k is the distance in meters measured down each leg from the beginning of that leg, as shown in Figure 5. (Note again that

notational differences exist between GO-71 and TE-82 concerning where to start measuring the distance in each leg: the former starts from the centerline of the previous leg; the latter starts after one is completely out of the previous leg. These distance coordinates differ by half the width of the previous leg; and are described in the tables in the Appendix as "centerline length" and "leg opening to mid-bend", respectively.) The factor $c_k = 1$ in general, except that it is set equal to two for the second leg of a labyrinth transmitting accelerator-produced neutrons because "the dose equivalent due to neutrons scattered into the second section is roughly a factor of 2 higher for accelerator-produced neutrons than for isotopic-source neutrons because of spectral differences" between the two sources. Clearly this is an approximaton valid only at distances greater than a meter or so into the second leg; at smaller distances the "attenuation" given by the above formula is greater than one.

One of the difficulties of using the Tesch results are that although they were obtained for labyrinths of two different cross sections (2.2 m x 1 m and 2.2 m x 2 m), the results are presented in terms of the distance in meters along the leg with the dependence on labyrinth cross section coming only from the factor $A^{1.3}$ in the second exponential. At distances large enough for the first exponential to be negligible, the rate of falloff of the DE with distance is independent of the labyrinth cross section. Further, at constant distance labyrinths of different cross sections have transmitted doses in ratios which depend only on the factors of $A^{1.3}$. Figure 10 shows the falloff of transmitted dose with distance as predicted by the Tesch and Goebel formulae for 30" and 60" diameter ducts and a 2 meter square passageway. Tesch's approach clearly has its limitations, especially for large distances and small duct cross sections. Nevertheless, these formulae were used with corrections for the source geometry (see below) to provide a second independent method of calculating the dose attenuation of the various RHIC labyrinths. I have taken rough agreement between these two methods as an indication of the correctness of their common prediction. Where they have disagreed, however, I have favored the Goebel result, but taken the disagreement between the methods as a warning that there should be a greater degree of uncertainty attached to the single number chosen.

The relative positions of the labyrinth opening and the beamline and loss point are critical to understanding the attenuation of the first leg. A "typical" cascade from a beam loss in a magnet extends perhaps 4 meters along the beam direction. Since most vents and labyrinths are 2 to 3 meters, and almost always less than 5 meters from the beamline, and a meter (vents) or two (personnel labyrinths) in width, it is clear that an actual beam loss distribution will more closely resemble a line source than an on-axis point source. For that part of the source which is off the axis of the first leg, a greater first-leg attenuation is to be expected. The calculations of Gollon and Awschalom (see Figure 7) show a first leg attenuation typically four times better for an isotropic line source than for an on-axis point source, although the exact difference in attenuation depends on the length of the leg. The "universal" curves of Goebel et al. show a smaller difference.

In a few cases, the mouth of the first leg lies at an elevation so far above the beamline that no neutrons emitted from a magnet can travel down the axis of the first leg without first scattering off the back wall of the tunnel. An example of this is shown as Figure 8. This situation is similar to that of the point source 45 degrees off axis as calculated by Gollon and Awschalom and shown in Figure 7. A similar effect is shown in Tesch's measurements , reproduced here as Figure 9, of an off-axis source position compared to an on-axis position for the same labyrinth used in the measurements leading to Equation (4). The attenuation for this situation can be an order of magnitude or more better than for a point source on axis, since when the source is far off the axis of

the first leg, that leg starts to attenuate like a second leg. The SAM-CE calculations reported by Goebel et al. [GO-75] show a similar effect in their Figure 3, but do not fall off as rapidly.

The preceeding discussion is most relevant when the the beam loss is known to be just upstream of the labyrinth entrance. The neutrons entering the labyrinth will then be primarily evaporation neutrons originating in the *magnets themselves at the cascade maximum*. When the loss point is not known, the labyrinth entrance dose and attenuation should be calculated using the loss location producing the highest transmitted dose. This will occur (A. J. Stevens, private communication) when the labyrinth is located at the point of *the cascade maximum along the accelerator tunnel wall*. At this point, the source of neutrons will be the omnidirectional "sea" of evaporation neutrons inside the accelerator enclosure coming from the cascade in the tunnel walls. This source term most closely resembles the "plane" sources of Goebel et al.

The effect of a distributed source is taken into account for all personnel labyrinths and air vents. In the Goebel method, this is done by using the formula (Equation 2) for a line or plane source. In the Tesch calculations, a "source geometry factor" is used to reduce the transmitted neutron flux below that predicted by the on-axis formula of Equation (4). The magnitude of this effect is somewhat arbitrarily taken to be 0.25 for all cases in which the beamline is within 25 degrees of the axis of the first leg, 0.15 for those cases in which the beamline is between 25 and 40 degrees, and 0.10 for larger angles. This is an oversimplification: the use of any single correction factor for a given angle will result in an overestimate of the tranmitted flux for long first legs, and an underestimate for short first legs.

The effect of a cul-de-sac or neutron trap at the end of a labyrinth leg has not been unequivocally determined. In both models, I have taken the maximum effect to be a reduction to 50% of the flux that would penetrate the labyrinth if the cul-de-sac were not there, when the depth of the cul-de-sac is equal to the square root of the cross sectional area of the labyrinth. This is a conservative assumption. For shorter cul-de-sacs, the effect was reduced proportionately. No such modifications have been made for the emergency ventilation shafts, which do not have cul-de-sacs.

The effect of neutron "punch-through" around the first two legs of a three-legged labyrinth was calculated by taking the star density at the accelerator tunnel wall, and extrapolating radially a distance equal to the length of the first leg to the wall at the second bend. The extrapolation was made using a RHIC tunnel CASIM calculation whose radial falloff was parametrized by Stevens [ST-92] as $C \exp(-r/r_0)/R^2$, where r is the shield thickness and R is the radial distance to the beamline, both in cm. The radial falloff parameter r_0 was found to be 67 cm in BNL soil in an "eyeball" fit to the CASIM results at large radii; see ST-92 figs. 2 and 3. At smaller radii the CASIM results generally fell above the fitted line. This was because the first few bins contain proton and pion produces stars; the fluxes of these particles die away quickly compared to the neutron flux [Stevens, private communication]. Extrapolating from the entrance dose using this model ignores the faster initial falloff shown in the CASIM runs, and thus produces an overestimate of the dose at large radii. The magnitude of this effect varied between the different geometries and runs made by Stevens, and the star density so calculated could therefore be as much as 50% too high, with a more likely figure being half that. In addition, uncertainties in the density of BNL soil can produce a systematic error of perhaps 15%.

This wall, a plane source of omnidirectional neutrons, was used as the source for a 1-leg labyrinth calculation. For convenience and conservatism, the Tesch on-axis (inverse square) formalism was used.

Circular Access Tunnel:

The only labyrinth which cannot be calculated using these methods is the circular access tunnel (case P-2) coming out of the transfer line from the AGS to RHIC. This tunnel has a central radius of 31.5 feet, a cross section of 7' wide x 8' high, and turns through 90 degrees. Circular access tunnels are hardly ever treated in the literature, since they are very rarely built. The only really satisfactory method is a full-scale Monte Carlo calculation.

Fortunately, such a calculation was made for a similar tunnel as part of a systematic study [GO-71]. The attenuation of a 90 degree tunnel of 27.5' central radius had been calculated for three cross sections having two different areas and aspect ratios. All transmitted fluxes were exponential in the bending angle θ: $H(\theta) = H(0) \exp(-\theta/\Lambda)$, where Λ was in the range of 9 to 12 degrees. For an aspect ratio of 2:1 (H:W), Λ could be parameterized as

$$\Lambda = 30\,(\sqrt{A}/R)^{0.625} \quad \text{(degrees)}$$

Scaling all dimensions by 86% to match the Monte Carlo calculation's radius of 27 ft yields an equivalent labyrinth of dimensions 6.9 ft by 6 ft, or an area A of 41.1 sq. ft. This yields an attenuation angle Λ of 12.2 degrees. After increasing the flux by a factor of two to account for the lesser effectiveness of a 1:1 aspect ratio [see Fig. 13 of GO-71], the resulting labyrinth attenuation is 1.25×10^{-3}.

The loss point for this labyrinth was taken to be the first magnet in the enclosure. At this point, the labyrinth itself is at an angle of 135^0 with respect to the beam, i.e. in the backwards hemisphere. Essentially all the dose at this location is low energy evaporation neutrons coming from the loss point and not obtainable directly from CASIM. I therefore assumed that the isotropic part of the dose (85%) at 45^0 (forward hemisphere) is also present in the backward hemisphere. To obtain this latter quantity I used Stevens' calculation of the star density on the wall of the transfer line enclosure for incident 10.4 GeV/u Au ions at 45^0 as a starting point. (The star density for this location was one third the star density at the peak of the cascade along the wall.) This was converted from stars per incident Au ion to stars per incident proton using the ratio of 125:1 obtained from figures 2 and 3 of ST-92. The dose incident on the tunnel entrance is then calculated to be 13 rem per AGS pulse of 2.4×10^{12} protons. The dose outside the tunnel entrance is then 32 mrem when two AGS pulses are lost in the tunnel on their way to RHIC.

Beam lost in the tunnel from the AGS at a point just upstream of the junction of this curved labyrinth with the transfer tunnel will produce neutrons which can penetrate the thin earth and concrete "wedge" and then propagate through the remaining portion of the accessway. The effect of this punchthrough was calculated to be1.5 mrem for two lost AGS pulses. For either loss situation, the dose outside the tunnel entrance will be limited by radiation activated interlocks which will limit the losses in the transfer line to at most two AGS pulses.

VI. DISCUSSION:

Quantities Calculated:

The necessary calculations were made using a spreadsheet program to facilitate revisions and documentation. The tables in the Appendix -- one per case for the personnel access labyrinths and ventilation ducts -- show all the input data, and the resulting labyrinth attenuation and exit dose in rem for the assumed loss scenarios. For each case, the dose rate incident on the labyrinth opening was calculated from the assumed loss scenario. In the case of the experimental halls, however, the number so calculated for an empty hall has minimal relation to the dose rate that would actually be present if a beam loss occurred in a hall filled with massive detectors.

The attenuation of each labyrinth was calculated from both the Tesch and Goebel formulas, and both results and their geometric mean are presented. In a number of cases the two methods agree extraordinarily well, being within 20 or 30% of one another. As a crude measure of the agreement of the two results, a "variance factor" is given: this is the number by which the geometric mean must be multiplied (divided) to obtain the larger (smaller) of the two results. Thus a variance factor of two means that both calculations yield results that are a factor of two away (one twice, the other half) from the stated geometric mean.

The geometric mean of these results is perhaps a better estimator of the actual attenuation than provided by either method by itself. Unless otherwise stated, it will be used as the basis for comparison with RHIC dose limits; when this is intended the numerical value of the geometrical mean is italicized. However, in a number of cases of exhaust vents (especially those with the smallest diameters) from the experimental halls, the Tesch formulas significantly underestimate the attenuation, and thus overestimate the transmitted dose. This results from two factors: first, the large size of the halls puts the supposed loss point some distance from the labyrinth opening, and thus Tesch's inverse square falloff from the source has only a small effect over the six foot length of the first leg. In addition, in the second legs Tesch does not take into account the fact that at large distances the dose falls off more rapidly in a 30 inch diameter duct than it does in a 60 inch duct or in a two meter accessway. This may be seen most readily in Figs. 10a and 10b. In such situations, the Goebel attenuation is indicated as being "preferred", and is italicized.

Finally, except in the case of experimental halls, the product of the incident dose rate and the labyrinth attenuation is presented as the "exit dose rate". In the case of the experimental halls, this is not a meaningful quantity, and is not thus given.

Radiation Protection Standards:

The RHIC SAD provides the following criteria for doses in unrestricted regions, and for regions which are restricted to "radiation workers":

Unrestricted Regions (Non-Radiation Workers):

	High Occupany	**Low Occupancy**
Normal Loss dose	<15 mrem/yr	<240 mrem/yr
Fault Loss Dose	<10 mrem/yr	<160 mrem/yr

Regions Restricted to Radiation Workers:

	High Occupany	Low Occupancy
Normal Loss dose	<0.2 mrem/hr	<3.2 mrem/hr
Fault Loss Dose	<500 mrem/yr	<1000 mrem/yr

In the above table, a "year" is defined as 2000 hours, which is taken to be the maximum amount of time an individual could spend in one location over the course of a year. "Low occupancy" is defined as 1/16 of this, or 125 hours per year, but not more than 1/2 hour per day. Regions which are not "low occupancy" must meet the more stringent "high occupancy" criteria. The area around an emergency exit in the middle of an empty field is considered a "low occupancy" area; the inside of a power supply building near the RHIC ring would be a "high occupancy" area.

Calculated Fault Losses at Personnel Access Labyrinths:

For all three-legged personnel access labyrinths, the assumed loss of the stored Au beam (RHIC) or two proton bunches during injection (Transfer Line) produces a dose outside the labyrinth of at most a few millirem. Many of these cases involve doses outside labyrinths such as emergency exits in isolated locations, where people are not expected to be in any case. For these labyrinths, the fault dose is obviously considerably below the 160 mrem/yr (interpreted as 160 mrem/fault) level permitted for unrestricted low occupancy areas. The curved access labyrinth, case P-2, with a calculated fault dose of 32 mrem is also below this level. All 3-leg labyrinths ending in "high occupancy" areas have fault doses calculated to be below 10 mrem.

The two legged labyrinths have poorer calculated neutron attenuations. The calculated additional dose equivalents due to the presence of the labyrinths under the same circumstances are higher, as shown below:

Case	Location	Calculated Fault DE	Variance Factor
P-11	10 O'clock to Service Bdlg	33 mrem	1.5
P-13	12 O'clock to Service Bdlg	50 mrem	2.6 Not As built See P-14
P-4	Eqt Areas 1A,1C,3A,3C Em. Exit	42 mrem	1.4

Since the first two of these terminate in Service Buildings, they cannot be considered as ending in low occupancy areas. The permitted fault dose for high occupancy areas is 10 mrem for unrestricted regions; for regions restricted to radiation workers, 500 mrem. Both of these regions are comfortably below the 500 mrem limit, but above the 10 mrem limit. *Thus, once the RHIC intensity approaches that given in the Design Manual* [and not the four times higher number used here, with an additional factor of two for an increase in the QF], *these two buildings will need to be treated as restricted areas because of their potential for doses resulting from fault doses.* The last of these ends in a field, and so the calculated DE falls below the permitted 160 mrem for a low-occupancy non-restricted area.

Another area of possible concern is the utility room with a wall in common with the third leg of case P-16, coming from the Transfer Line. The fault DE is 0.75 mrem, with the last leg providing attenuationto the outside world of 0.025 or 0.050, according to the model employed. This attenuation is lost when neutrons go from the second leg into the utility room. However, this is essentially made up by the attenuation of the neutrons going through the foot-thick concrete wall between the labyrinth and the utility room: 30 cm of concrete provides attenuation of 0.05 or 0.022 for 5 MeV and 2.5 MeV neutrons, respectively [NBS-63, figs 4B and 5B]. Thus the dose in the utility room is no worse than at the labyrinth exit, and falls below the applicable limit.

It is also worth noting that some of the regions around the personnel accesses or emergency exits are thinly shielded. Perhaps the worst example is at Equipment Areas 1A, 1C, 3A, and 3C. The cavity for the helium expansion loop has only eight feet of earth shielding shown on the drawing. In addition, in the direction of the door from the emergency exit, there is a spot with only ten feet of earth shielding in the radial direction. *These areas need to be looked at with some care.*

Calculated Fault Losses at Ventilation Ducts:

The two legged air shafts have poorer attenuation, with calculated exit doses of some tens of millirem up past two hundred millirem. The vents with the higher levels are shown below:

Case	Location	Calculated Fault DE	Variance Factor
V-6	Eqt Area 1A, 1C, 3A, 3C	141 mrem	1.89
V-7	*Magnet Encl Sextant 1*	*201*	*1.10*
V-11	*Tunnel bet. Eqt Areas 3A & 3B*	*222*	*1.06*
V-17	Next to Open Area 4 O'clock	128	1.32
V-18	CW from Open Area to Support Bdlg	128	1.32
V-19	CCW from Open Area	128	1.32
V-22	*Eqt Area Emgcy Exit 5A*	*235*	*1.58*
V-23	Magnet Encl near Exit to Service Bdlg	140	1.23
V-26	*West Injection Structure*	*227*	*1.23*
V-29	MFH 8 o'clock to support bdlg	106	1.22

Four of these vents have calculated fault levels in excess of the 160 mrem permitted for an uncontrolled low access area. The calculations themselves represent the average dose rate over the pipe area at the point at which the pipe emerges from the ground. Since most of the neutrons streaming up the vent are moving approximately parallel to its axis, the dose over the top of the vent pipe will also be close to this value. The angular distribution of neutron velocities at the end of the second leg (taken from VO-75 figure 9) was used to determine the highest dose at the vertical sides of the pipe. This was found, at a level two to three feet above the ground, to be *approximately one third of the number quoted above.* If we consider the area of concern to be the closest readily accessible area - the side of the vertical duct pipe - then all the above numbers are reduced by a factor of three, *and then all fall within the low occupancy unrestricted criterion of 160 mrem/fault.*

In addition, these calculatons are based on an assumed RHIC intensity four times higher than that of the Design Manual, and include an additional factor of two to allow for a higher QF. *These regions can thus be allowed to remain unfenced at the time of RHIC startup.* There will then

be plenty of time to make measurements around the vent from the Transfer Line, case V-3, where measurable losses will occur on a routine basis, in order to validate the methodology used here. Even if the controlling location is taken to be the hot spot directly over the vent shaft, *the results of those measurements can still be used to better determine which vents, if any, need to be fenced before the RHIC intensity approaches the basis used for this calculation.*

The areas next to several of the ventilation ducts on the side away from the RHIC tunnel are very thinly shielded. These areas are the various A, B and C equipment areas. The presence of the vent which emerges from a point high on the enclosure wall (see Fig. 8) results in there being a small area which has only a few feet of earth in a line of sight to the magnets. *The adequacy of the shielding at these points needs further checking.*

Calculated Chronic losses in the Transfer Line:

As stated earlier, if the largest chronic loss of 0.05% occurred at the same location for a full year's operation of the Transfer Line, the resulting dose outside the shielding would be about 18 times greater than that resulting from the fault loss of two pulses of 2.4×10^{12} protons at 28 GeV/c. The resulting doses outside the four penetrations into the Transfer Line are:

Case	Location	Calculated Chronic DE	Variance Factor
V-3	*Injection line at AGS to RHIC transition*	*855 mrem/year*	*1.12*
P-1	Injection line at AGS to RHIC transition	2.2	2.
P-2	*Curved Entryway to Transfer Line*	*590*	--
P-16	Fork in U-line near Neutrino Tunnel	14	1.02

Two of these locations (V-3 vent and P-2 curved labyrinth) have chronic dose rates substantially greater than the 240 mrem/year permitted in low occupancy unrestricted locations. ***At a minimum, these areas should be monitored for their actual radiation levels.*** In addition, unless the actual percent Transfer Line losses turn out to be less than a third of the anticipated losses there, *these locations will have to be protected in some way (shielding blocks, fences) when the current injected into RHIC becomes twice the Design Manual value.*

VII. ACKNOWLEDGEMENT:

This work would not have been finished without the continued encouragement of Steve Musolino or the critical discussions, comments and assistance of Alan Stevens.

REFERENCES

AR-69. T. W. Armstrong and R. G. Alsmiller, Jr. ORNL-TM-2498 (1969).

BNL-90. RHIC Design Manual, Revision 0. Brookhaven National Laboratory, October 1990.

CO-85. J.D. Cossairt, J. G. Couch, A. J. Elwyn, and W. S. Freeman, "Radiation Measurements in a Labyrinth Penetration at a High Energy Proton Accelerator", Health Physics 49 907-917 (1985).

DOE-92. U. S. Department of Energy Radiological Control Manual, Washington, D. C., USDOE Report No. N5486.6, June 1992.

GE-68. "Variante du Programme ZEUS Applique a des Problemes de Tunnels", C. E. N. Fontenay-aux-roses, Note CEA-N-933 (1968).

GO-71. Peter J. Gollon and M. A. Awschalom, "Design of Penetrations in Hadron Shields", IEEE Trans. Nucl. Sci. NS-18 741 (1971). Also appears in a longer form in Proc. Intl. Conf. Protection against Accel. and Space Radiation, CERN 71-16, pp. 697-713 (1971).

GO-75. K. Goebel, G. R. Stevenson, J. T. Routti and H. G. Vogt, "Evaluating Dose Rates Due to Neutron Leakage Through the Access Tunnels of the SPS", CERN LABII-RA/Note/75-10 (1975).

GO-76. Peter J. Gollon, "Dosimetry and Shielding Factors Relevant to the Design of Iron Beam Dumps", Fermilab TM-664 (1976).

GO-78. Peter J. Gollon, "Electronics in the Isabelle Tunnel", BNL Isabelle Technical Note 82.

GO-84. Peter J. Gollon and W. Robert Casey, "Isabelle Shielding Criteria and Design", Health Physics 46, 123-132 (1984).

HA-92. M. Harrison and A. J. Stevens, "Beam Loss Scenario at RHIC", AD/RHIC/RD-52, January 1993.

NBS-63 "Protection Against Neutron Radiation up to 30 Million Electron Volts", U.S. N.B.S. Handbook 63, April 1967.

RO-75. J. T. Routti and M. H. Van De Voorde, "Estimates of Neutron Leakage Through Penetrations of the CERN Intersecting Storage Rings by Monte Carlo Albedo Calculatons", Nucl. Eng. and Design 34 293-305 (1975).

ST-86. G. R. Stevenson, "Dose Equivalent per Star in Hadron Cascade Calculations", CERN Report TIS-RP/173, May 1986.

ST-87. Alan J. Stevens, "Radioisotope Production in air and soil in RHIC", BNL AD/RHIC-29 (1987)

ST-87b. G. R. Stevenson, "Neutron Attenuation in Labyrinths, Ducts and Penetrations at High-Energy Proton Accelerators", CERN TIS-RP/182/CF, 5 January 1987; paper presented to ANS Topical Conference on Theory and Practices in Radiation Shielding, Knoxville, TN, 22-24 April, 1987.

ST-87c. Graham R. Stevenson and Alberto Fasso. "A Comparison of a MORSE Calculation of Attenuation in a Concrete-Lined Duct with Experimental Data from the CERN PS". CERN TIS-RP/185/CF (1987).

ST-88. G. R. Steveson, "Dose Eqivalent Per Star in Hadron Cascade Calculations", CERN Report TIS-RP/173 (1988).

ST-90. Alan J. Stevens, private communication.

ST-92. Alan J. Stevens, "Analysis of Radiation Levels Associated with Operation of the RHIC Transfer Line", Draft Version 5, 9/28/92

ST-92b. Alan J. Stevens, "Local Shielding Requirements for the STAR Detector", RHIC/DET Note 5, 1992.

ST-94. Alan J. Stevens, "An Approximate Method for Evaluating Neutron Punch Through in Certain Classes of Shielding Penetrations", AD/RHIC/RD-65, January 1994. Note that Stevens discussion divides this component into two components according to the type of radiation they represent (*high energy particles* which would not have exited the shield if it had not been weakened by the penetration, and *evaporation neutrons* from the wall of the penetration), and does not directly address the radiation streaming down the penetration. Thus his components are not the same as those discussed here.

TE-82. K. Tesch, "The Attenuation of the Neutron Dose Equivalent in a Labyrinth through an Accelerator Shield", *Particle Accelerators* 12, 169-175 (1982)

VA-75. A. Van Ginneken, "CASIM: Program to Simulate Transport of Hadronic Cascades in Bulk Matter", Fermilab Report FN-72 (1975).

VO-75. H. G. Vogt. "Monte Carlo Calculations of the Neutron Transmission Through the Access Ways of the Cern Super Proton Synchrotron", CERN 75-14 (1975).

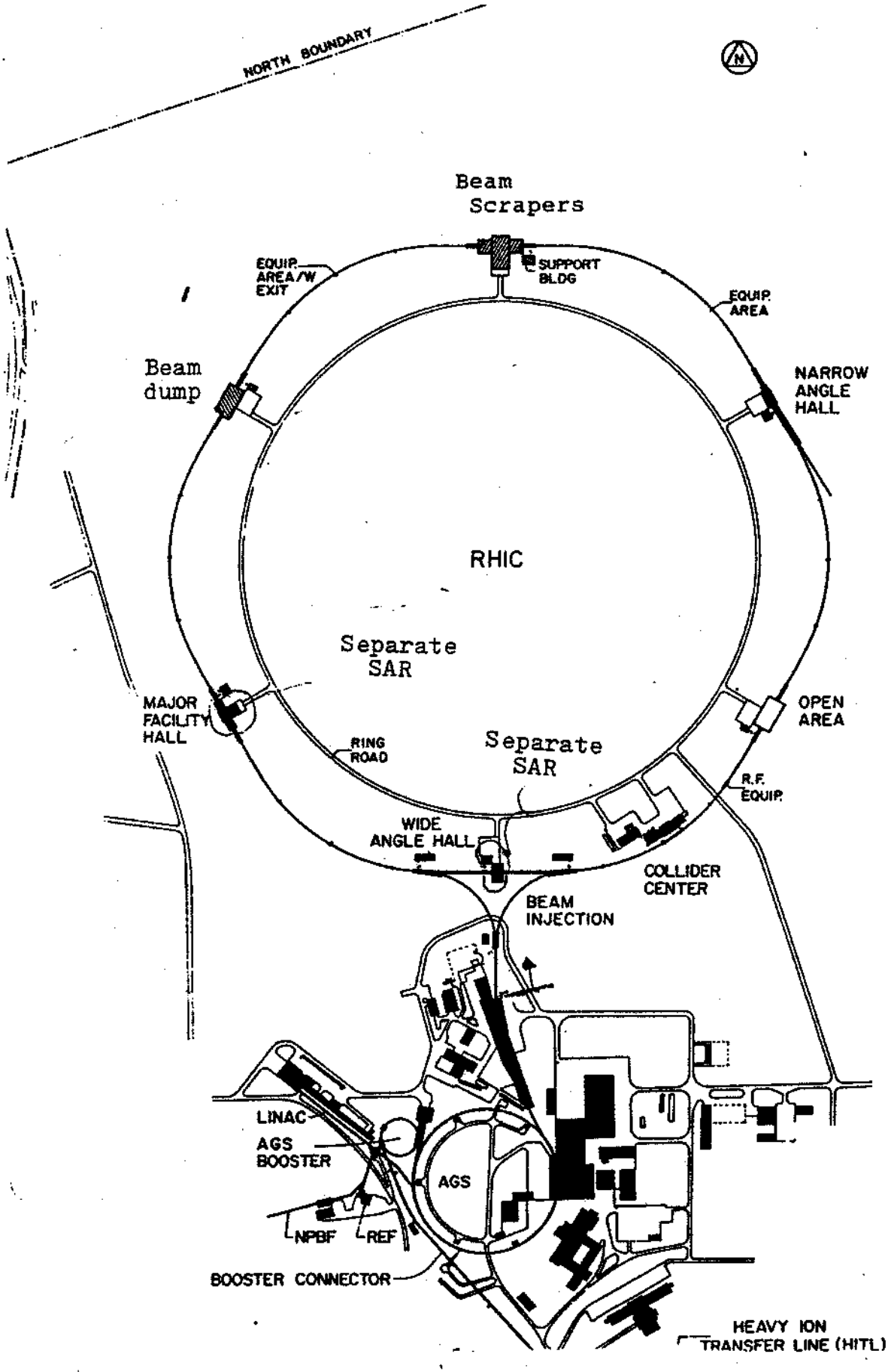

FIGURE 1. Layout of the RHIC Collider in relation to the AGS and transfer line.

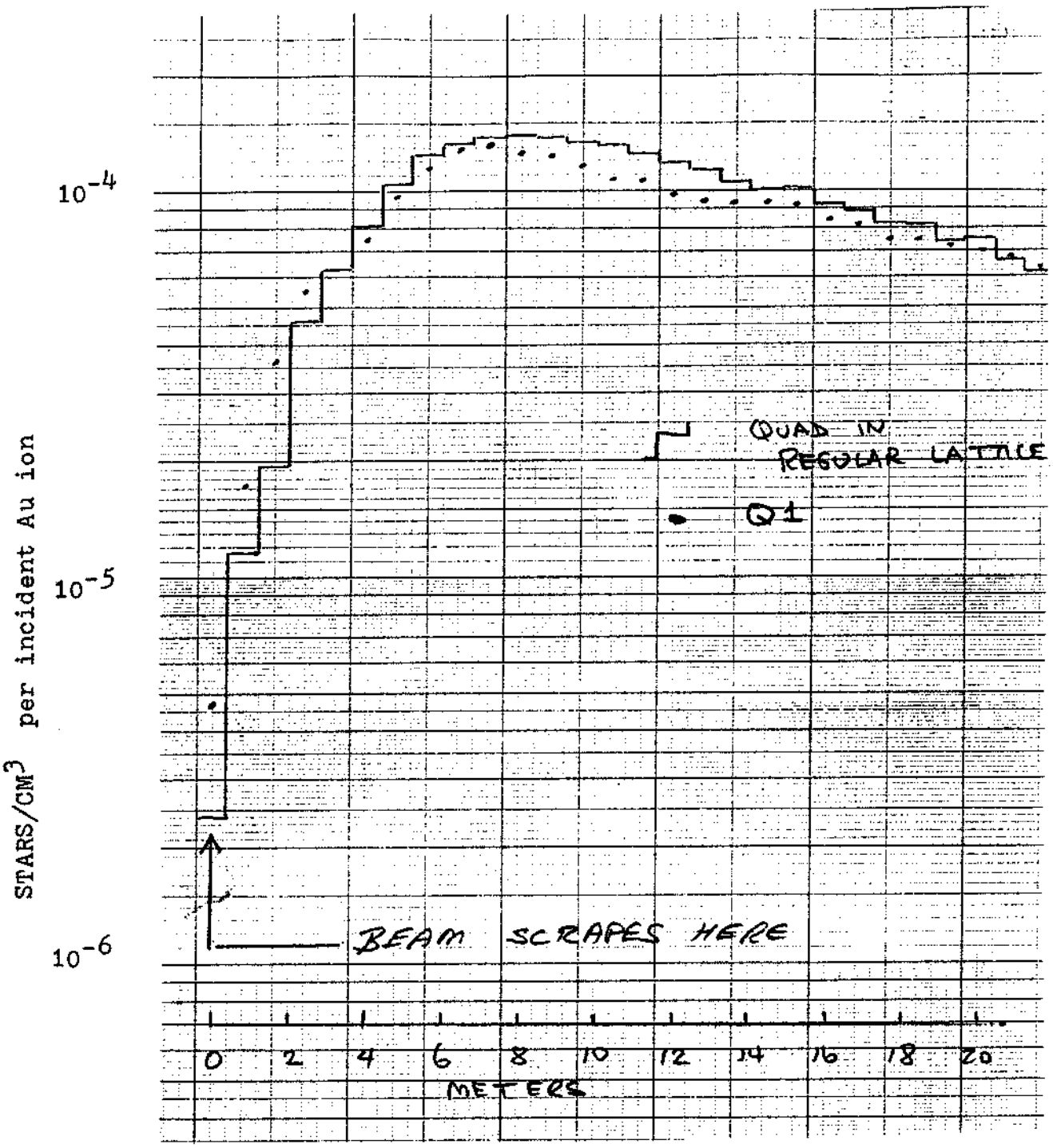

FIGURE 2. Star density at inside of magnet enclosure wall as a function of distance from loss point, according to a calculation by A. J. Stevens using CASIM. The incident beam was 100 GeV/u Au ions. The enclosure wall was taken to be soil at a radius of 2.5 meters.

Cossairt et al.
Health Physics 49
907-917 (1985)

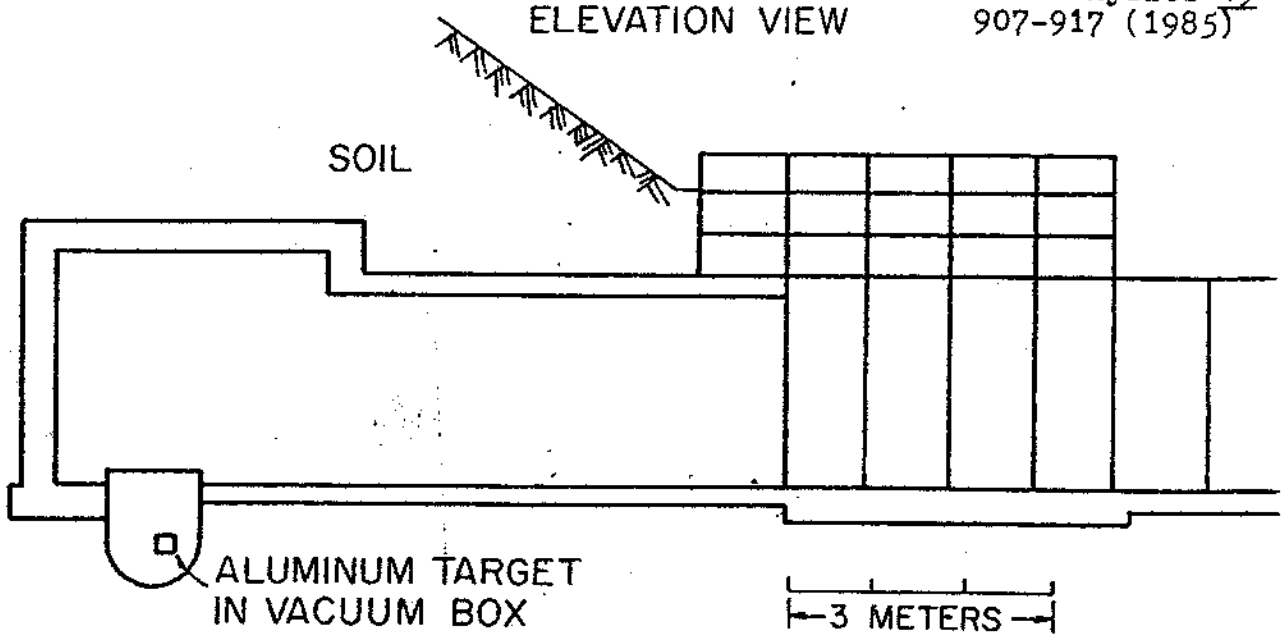

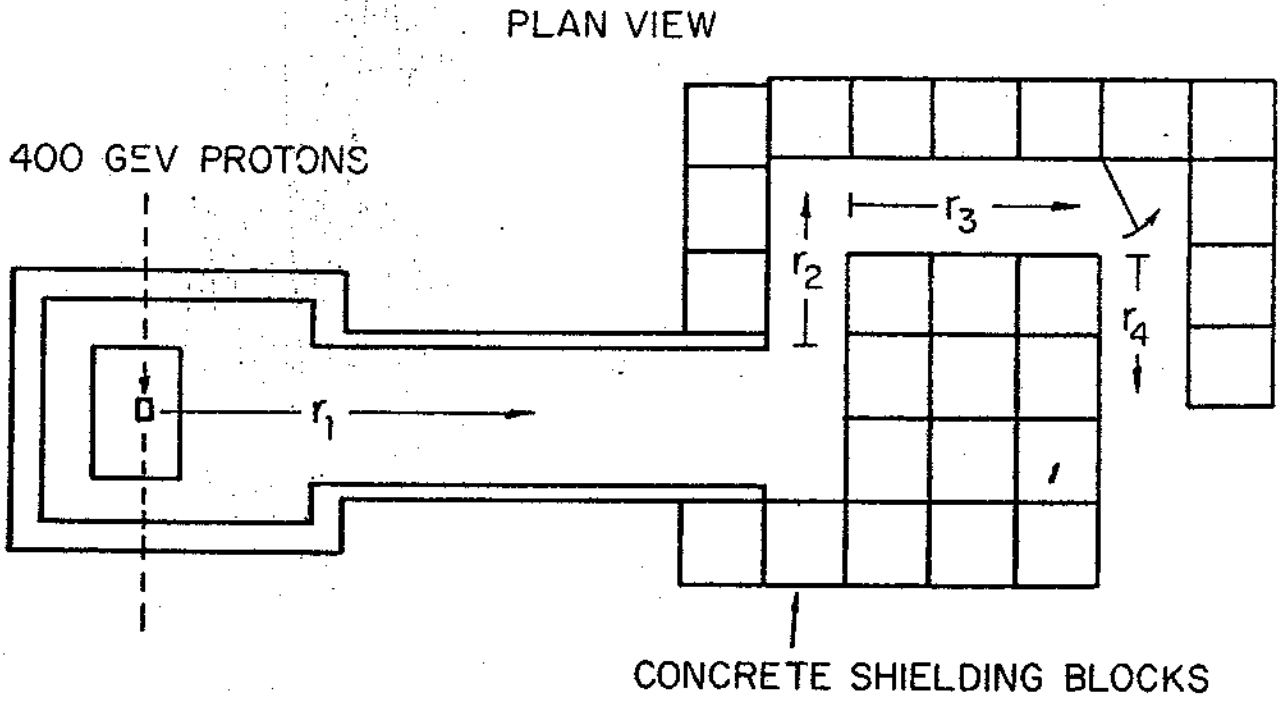

FIGURE 3. Geometry of absorbed dose measurements made by Cossairt et al. at Fermilab (Health Physics 49, 907-917 1985).

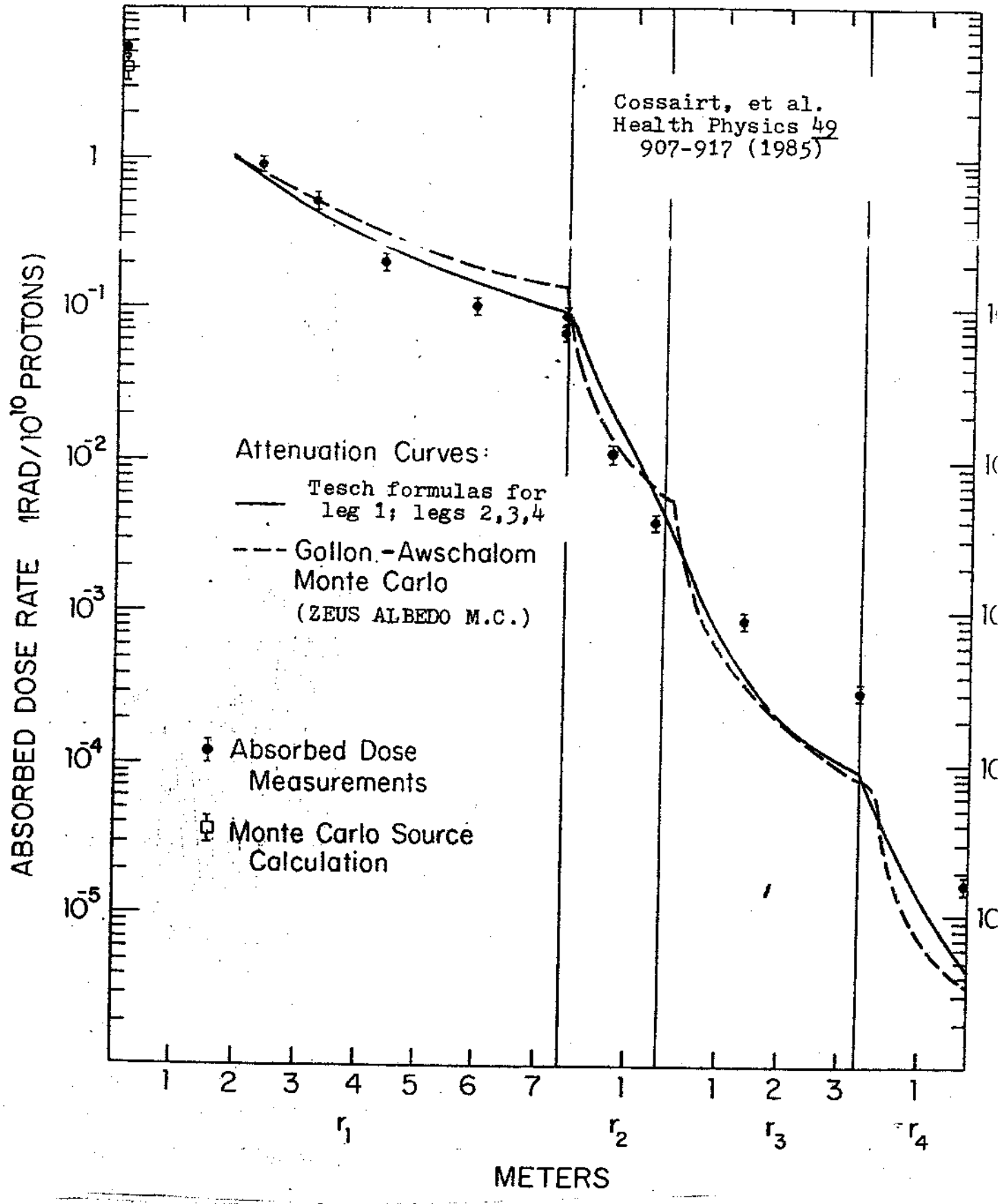

FIGURE 4. Results of absorbed dose measurements made by Cossairt et al., with comparison to Monte Carlo calculations of Awschalom and Gollon, and the parameterization of Tesch used in this Report.

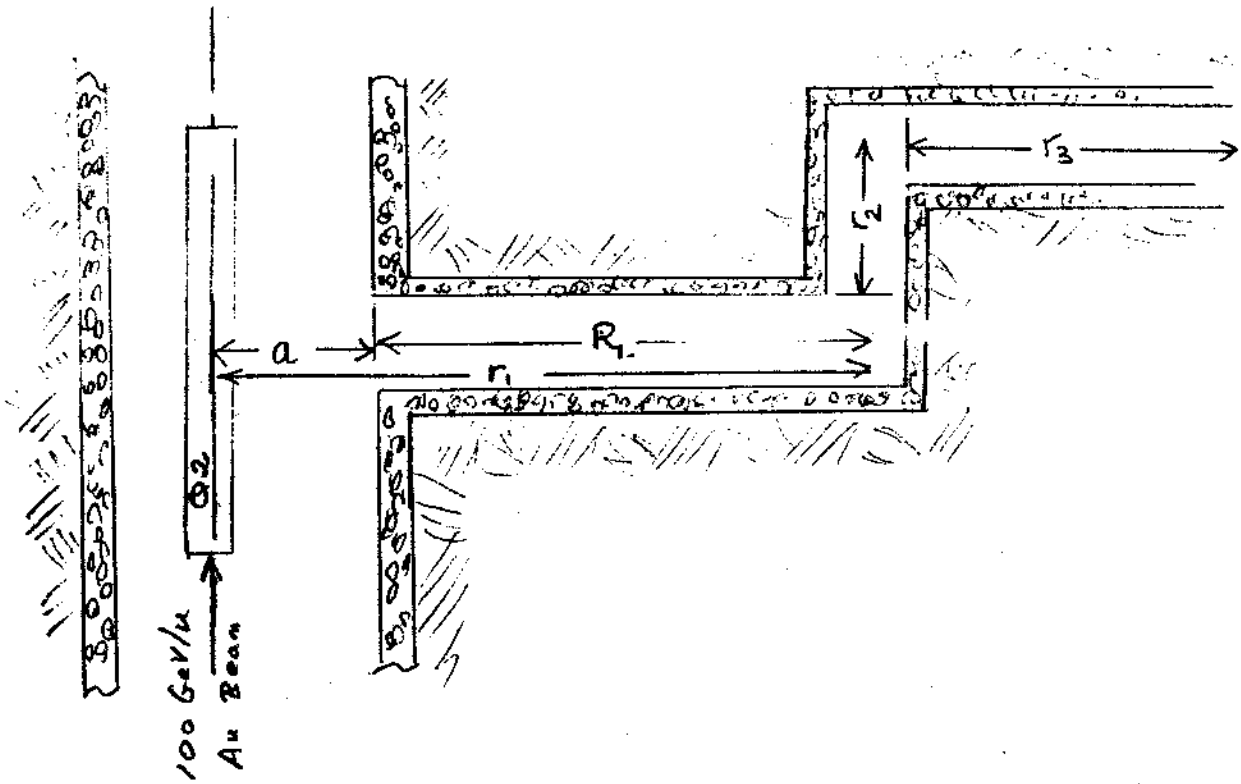

FIGURE 5. Notation used in this report for tunnel radius and length of labyrinth legs.

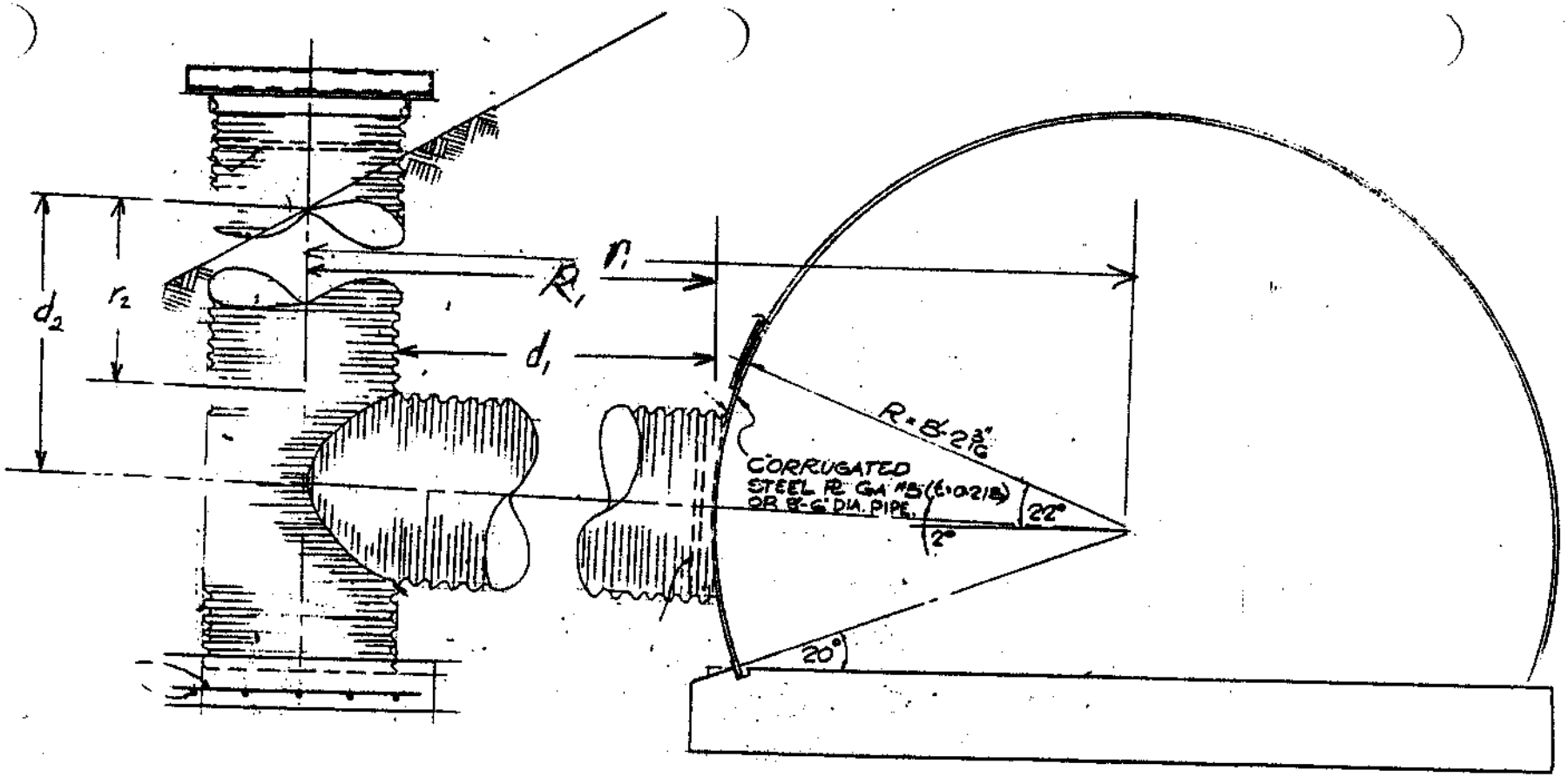

FIGURE 6. A typical ventilation duct in a plate arch tunnel structure. The vent diameter is 42, 48, or 54 inches, depending on location. The distance d11, measured from the outside of the tunnel enclosure to the closest point of the vertical pipe, is always 6 feet. The "proper" length R11 of the first duct leg includes the tunnel wall thickness, important when the wall is concrete instead of plate arch. The "Tesch" length of the first leg, r11, is measured from the beamline to the centerline of the bend.

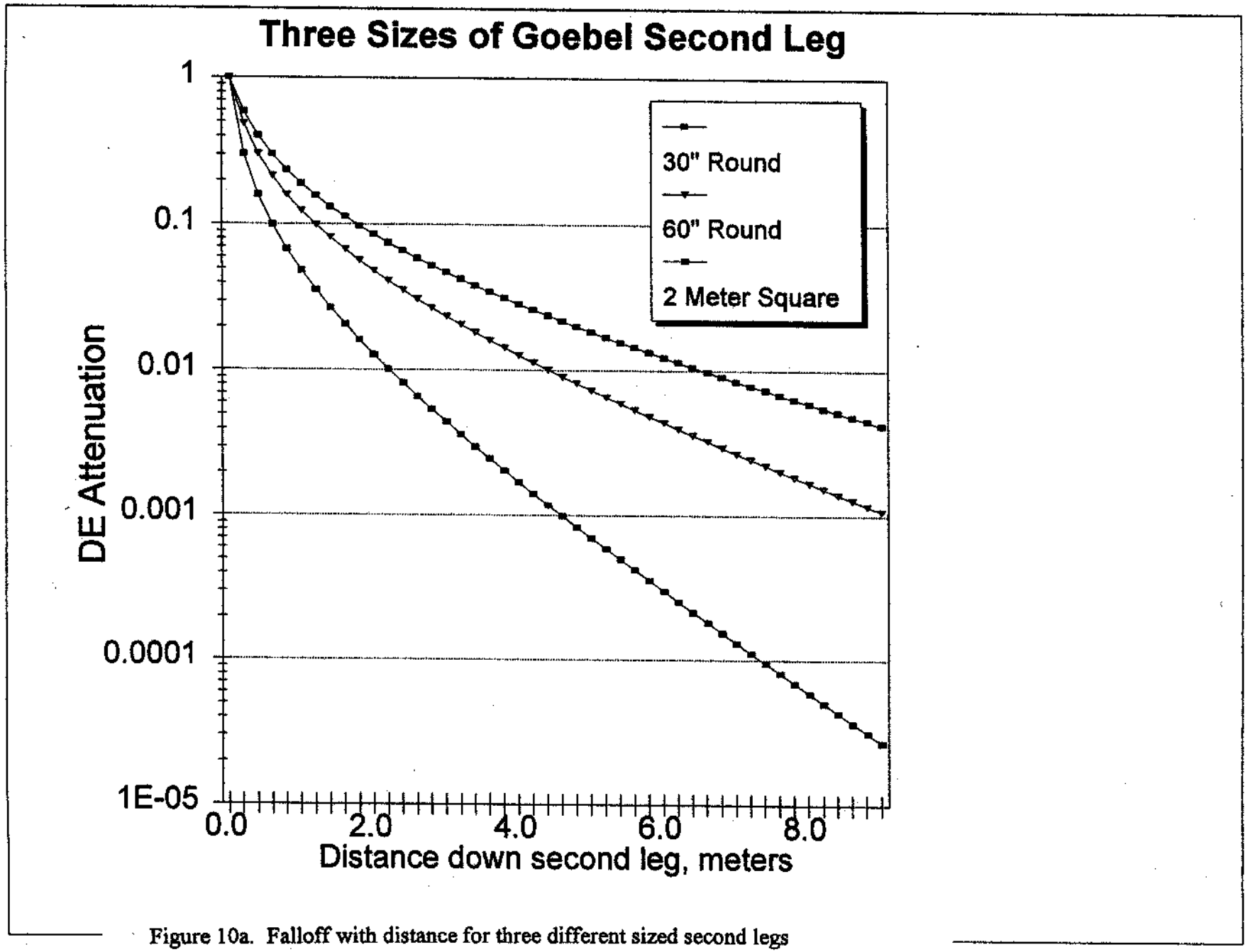

Figure 10a. Falloff with distance for three different sized second legs according to parametrization of Goebel results.

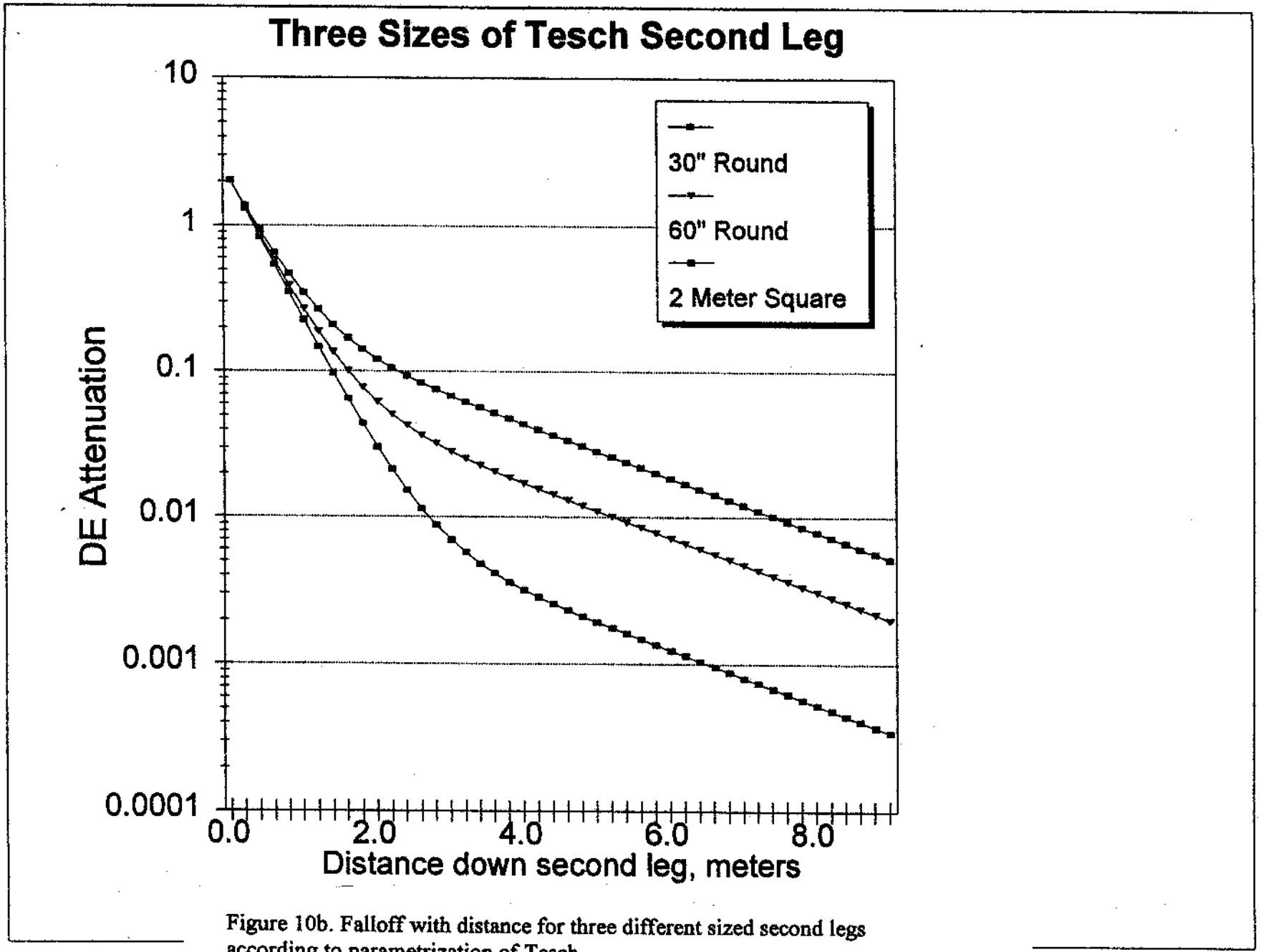

Figure 10b. Falloff with distance for three different sized second legs according to parametrization of Tesch.

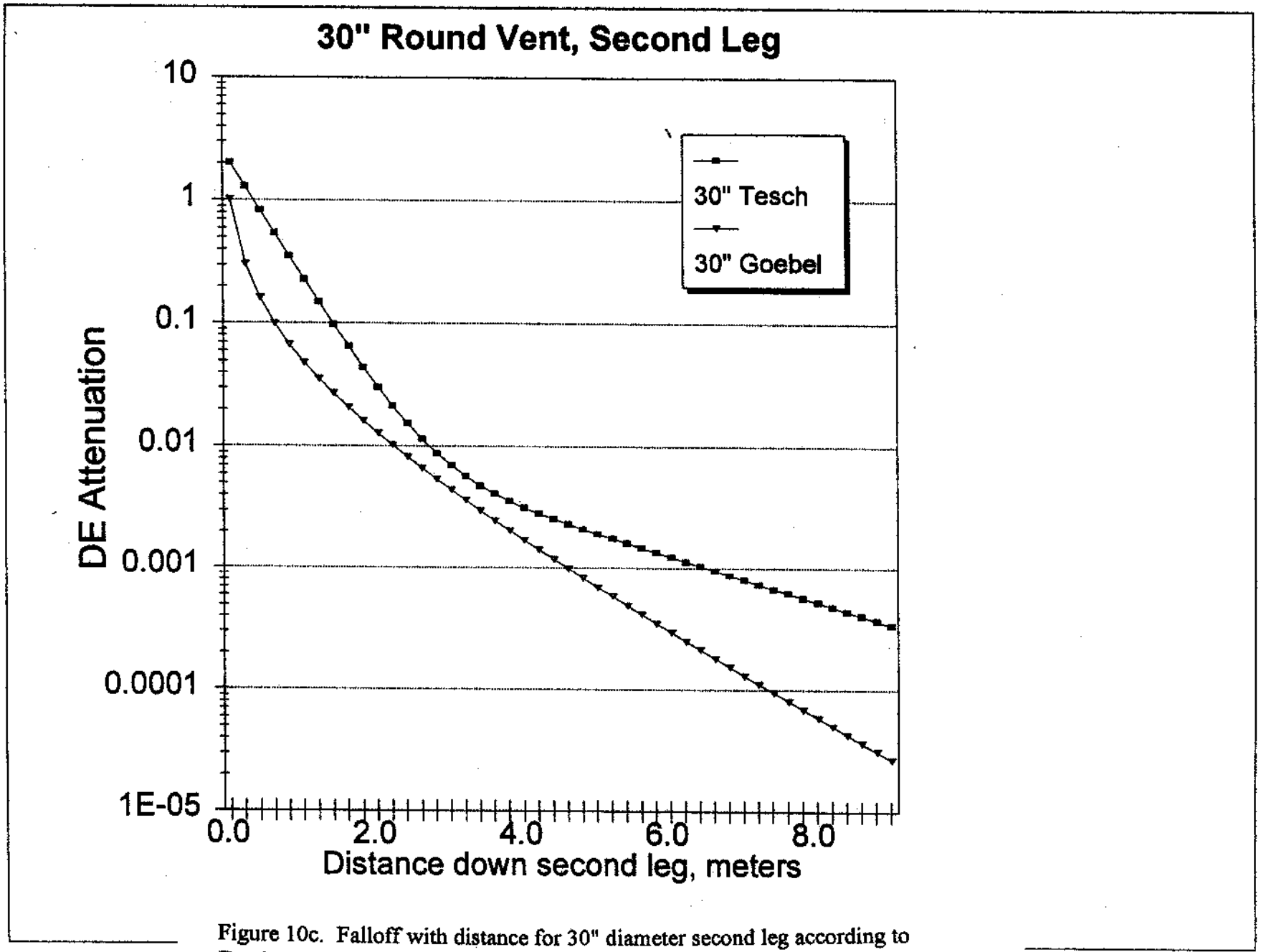

Figure 10c. Falloff with distance for 30" diameter second leg according to Tesch and Goebel parameterizations.

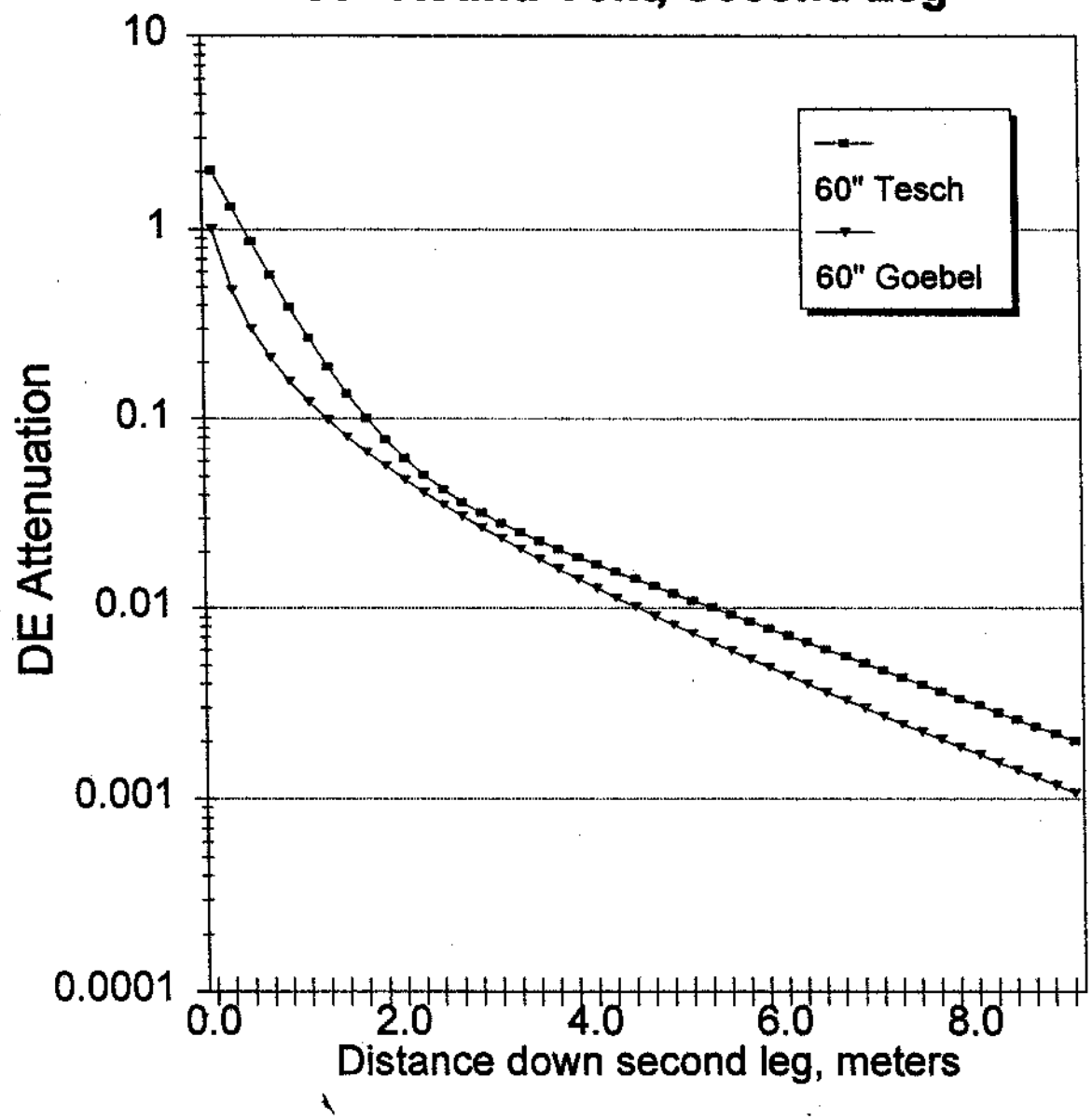

Figure 10d. Falloff with distance for 60" diameter second leg according to Tesch and Goebel parameterizations.

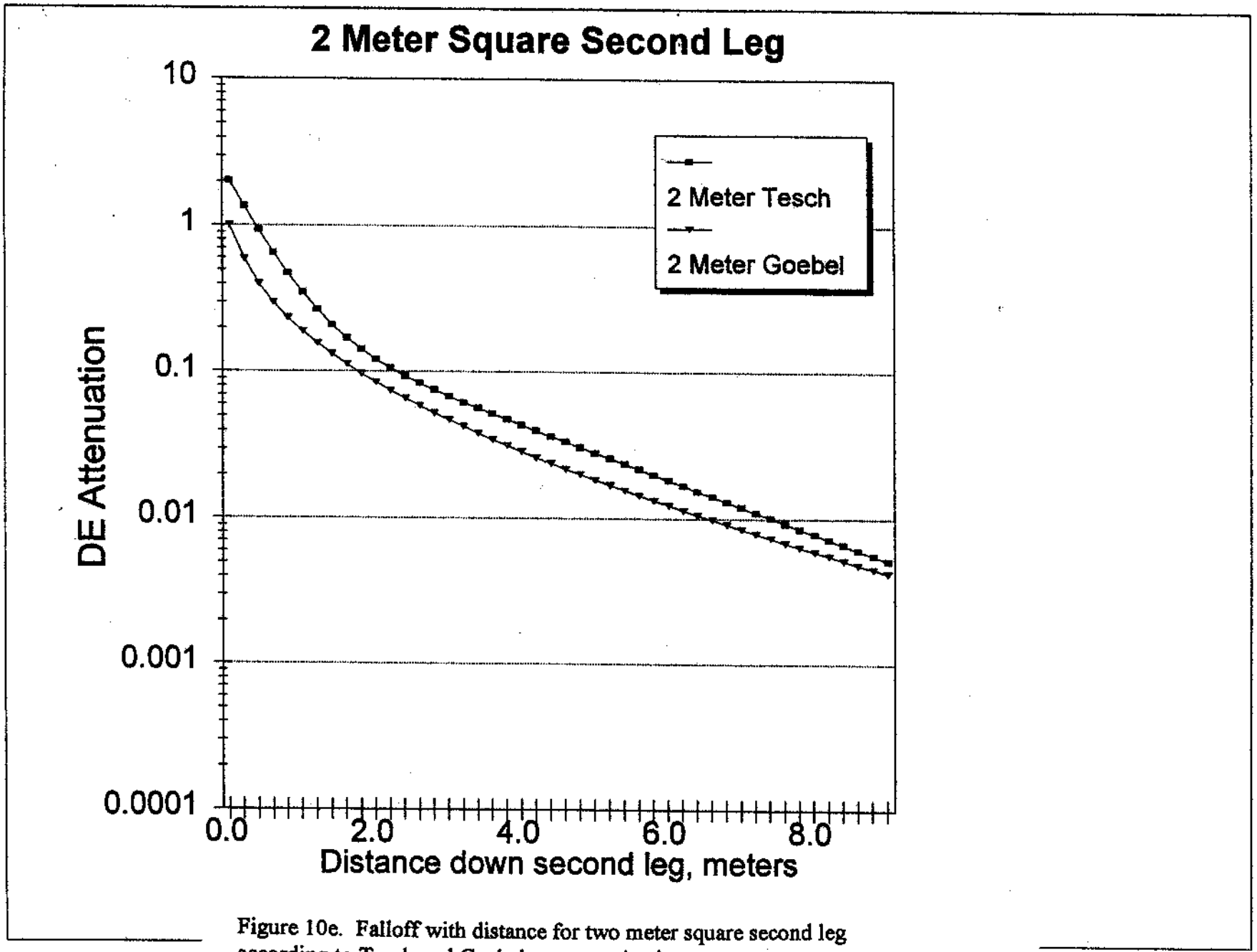

Figure 10e. Falloff with distance for two meter square second leg according to Tesch and Goebel parameterizations.

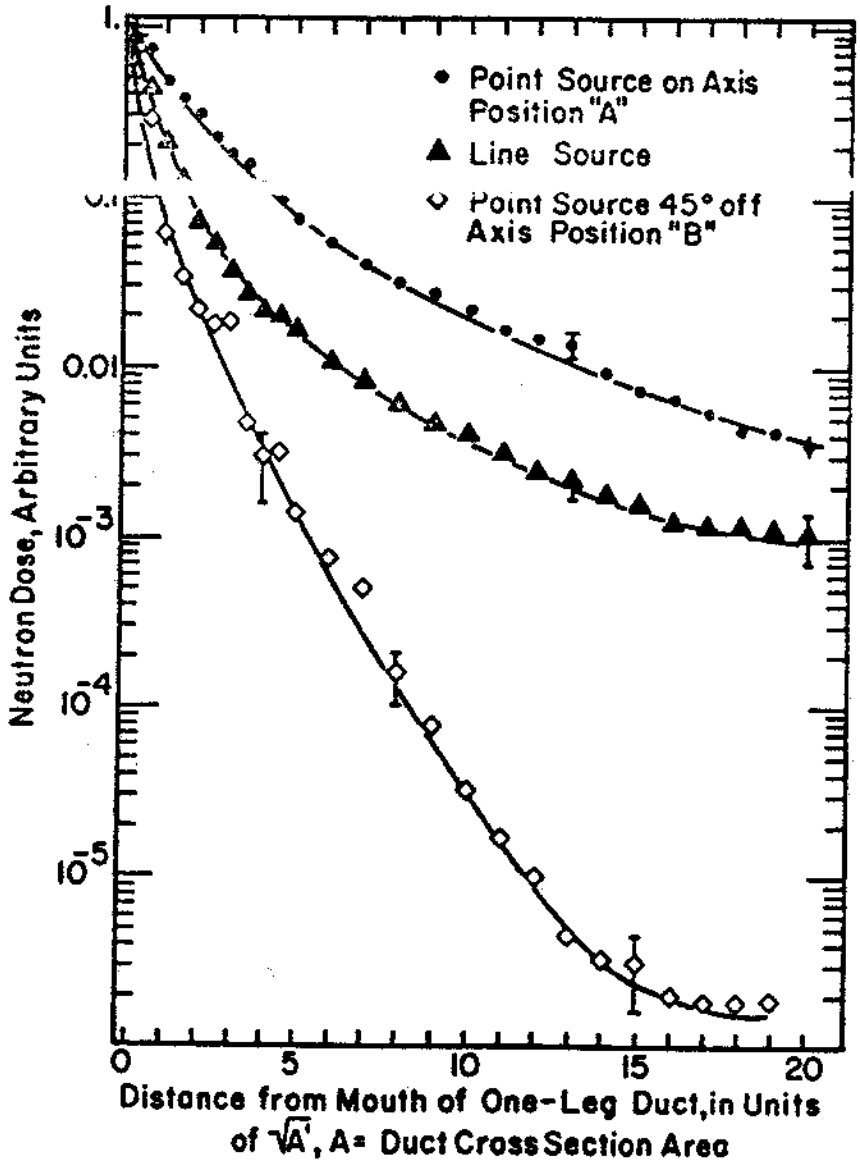

FIGURE 7. Calculated neutron dose in a straight penetration with a 2:1 aspect ratio for different neutron source locations. (Taken from Gollon and Awschalom, GO-71.) Note that different notation is used in this figure: distance down the first leg is measured in units of the square root of the cross secion area, starting from the point where the labyrinth joins the accelerator enclosure.

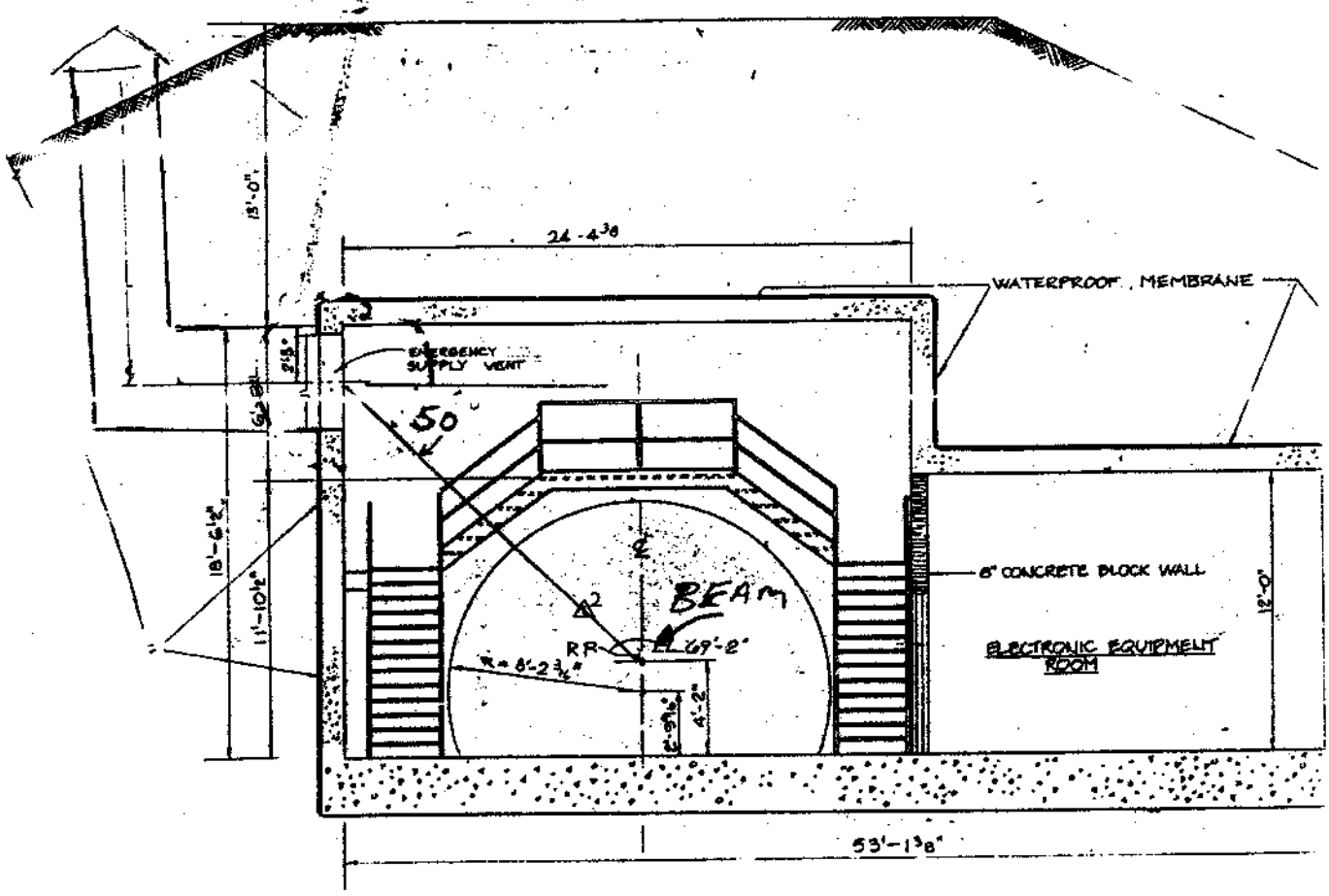

FIGURE 8. The ventilation duct at Equipment Area 7-B, showing the elevation of the duct above the beamline.

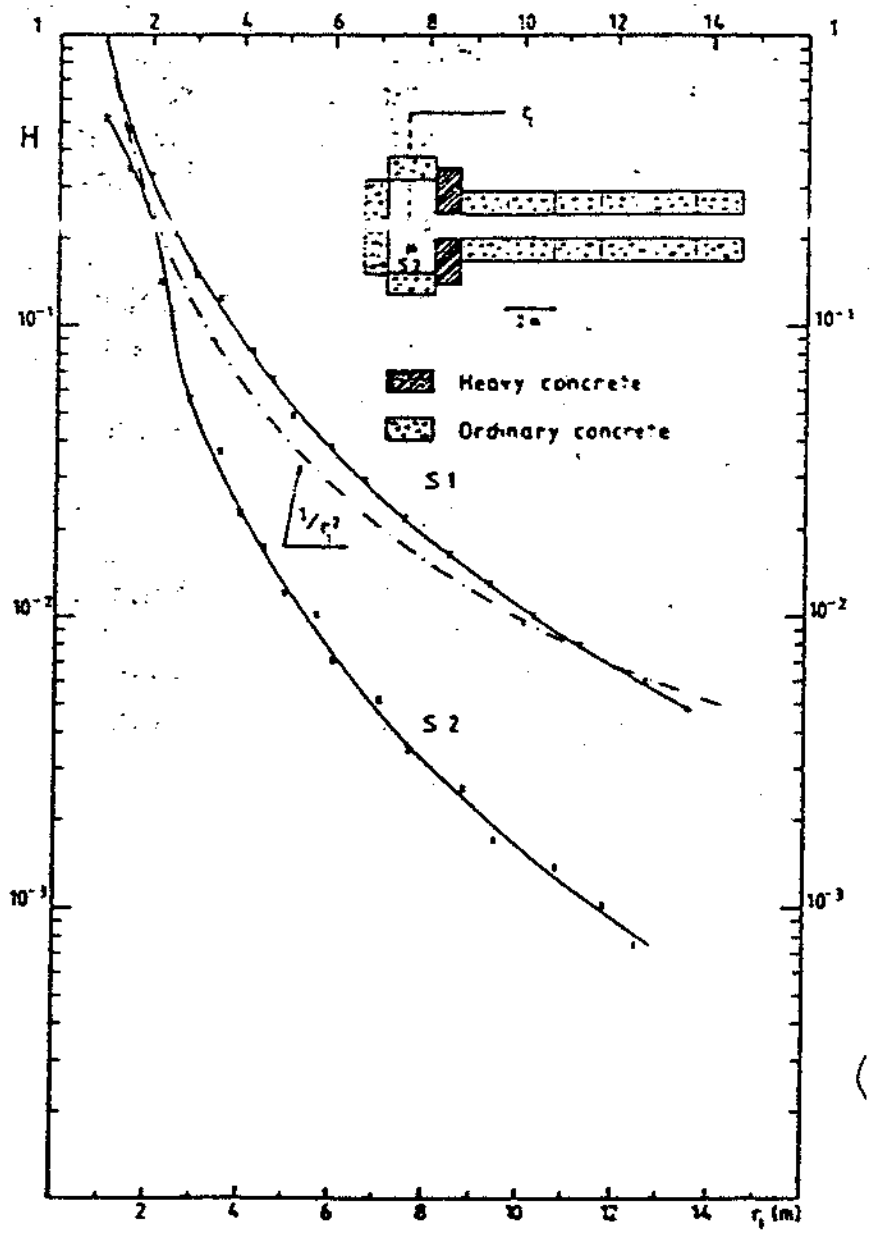

FIGURE 9. Neutron attenuation in the first leg of a duct for on-axis source position (S1) and off-axis source position (S2), as measured by Tesch [TE-82]